2. **Chang J, et al.** 2004. miR-122, a mammalian liver-specific microRNA, is processed from hcr mRNA and may downregulate the high affinity cationic amino acid transporter CAT-1. RNA Biol. **1**:106–113.
3. **Chenna R, et al.** 2003. Multiple sequence alignment with the Clustal series of programs. Nucleic Acids Res. **31**:3497–3500.
4. **Combet C, et al.** 2007. euHCVdb: the European hepatitis C virus database. Nucleic Acids Res. **35**:D363–D366.
5. **Crooks GE, Hon G, Chandonia JM, Brenner SE.** 2004. WebLogo: a sequence logo generator. Genome Res. **14**:1188–1190.
6. **Davis GL, Alter MJ, El-Serag H, Poynard T, Jennings LW.** 2010. Aging of hepatitis C virus (HCV)-infected persons in the United States: a multiple cohort model of HCV prevalence and disease progression. Gastroenterology **138**:513–521.
7. **Edgar RC.** 2004. MUSCLE: multiple sequence alignment with high accuracy and high throughput. Nucleic Acids Res. **32**:1792–1797.
8. **Fabian MR, Sonenberg N, Filipowicz W.** 2010. Regulation of mRNA translation and stability by microRNAs. Annu. Rev. Biochem. **79**:351–379.
9. **Friebe P, Lohmann V, Krieger N, Bartenschlager R.** 2001. Sequences in the 5′ nontranslated region of hepatitis C virus required for RNA replication. J. Virol. **75**:12047–12057.
10. **Fukushi S, et al.** 2001. Interaction of poly(rC)-binding protein 2 with the 5′-terminal stem loop of the hepatitis C-virus genome. Virus Res. **73**:67–79.
11. **Galtier N, Gouy M, Gautier C.** 1996. SEAVIEW and PHYLO_WIN: two graphic tools for sequence alignment and molecular phylogeny. Comput. Appl. Biosci. **12**:543–548.
12. **Grimson A, et al.** 2007. MicroRNA targeting specificity in mammals: determinants beyond seed pairing. Mol. Cell **27**:91–105.
13. **Hafner M, et al.** 2010. Transcriptome-wide identification of RNA-binding protein and microRNA target sites by PAR-CLIP. Cell **141**:129–141.
14. **Henke JI, et al.** 2008. microRNA-122 stimulates translation of hepatitis C virus RNA. EMBO J. **27**:3300–3310.
15. **Jangra RK, Yi M, Lemon SM.** 2010. miR-122 regulation of hepatitis C virus translation and infectious virus production. J. Virol. **84**:6615–6625.
16. **Jopling CL, Schutz S, Sarnow P.** 2008. Position-dependent function for a tandem microRNA miR-122-binding site located in the hepatitis C virus RNA genome. Cell Host Microbe **4**:77–85.
17. **Jopling CL, Yi M, Lancaster AM, Lemon SM, Sarnow P.** 2005. Modulation of hepatitis C virus RNA abundance by a liver-specific microRNA. Science **309**:1577–1581.
18. **Lemon SM, Walker C, Alter MJ, Yi M.** 2007. Hepatitis C viruses, p 1253–1304. *In* Knipe DM, et al (ed), Fields virology, 5th ed. Lippincott Williams & Wilkins, Philadelphia, PA.
19. **Ma Y, Yates J, Liang Y, Lemon SM, Yi M.** 2008. NS3 helicase domains involved in infectious intracellular hepatitis C virus particle assembly. J. Virol. **82**:7624–7639.
20. **Machlin ES, Sarnow P, Sagan SM.** 2011. Masking the 5′ terminal nucleotides of the hepatitis C virus genome by an unconventional microRNA-target RNA complex. Proc. Natl. Acad. Sci. U. S. A. **108**:3193–3198.
21. **O'Carroll D, et al.** 2007. A Slicer-independent role for Argonaute 2 in hematopoiesis and the microRNA pathway. Genes Dev. **21**:1999–2004.
22. **Pang PS, et al.** 2012. Structural map of a microRNA-122: hepatitis C virus complex. J. Virol. **86**:1250–1254.
23. **Perz JF, Armstrong GL, Farrington LA, Hutin YJ, Bell BP.** 2006. The contributions of hepatitis B virus and hepatitis C virus infections to cirrhosis and primary liver cancer worldwide. J. Hepatol. **45**:529–538.
24. **Roberts AP, Lewis AP, Jopling CL.** 2011. miR-122 activates hepatitis C virus translation by a specialized mechanism requiring particular RNA components. Nucleic Acids Res. **39**:7716–7729.
25. **Shimakami T, et al.** 2011. Protease inhibitor-resistant hepatitis C virus mutants with reduced fitness from impaired production of infectious virus. Gastroenterology **140**:667–675.
26. **Shimakami T, et al.** 2012. Stabilization of hepatitis C RNA by an Ago2-miR-122 complex. Proc. Natl. Acad. Sci. U. S. A. **109**:941–946.
27. **Simmonds P, et al.** 2005. Consensus proposals for a unified system of nomenclature of hepatitis C virus genotypes. Hepatology **42**:962–973.
28. **Villanueva RA, et al.** 2010. miR-122 does not modulate the elongation phase of hepatitis C virus RNA synthesis in isolated replicase complexes. Antiviral Res. **88**:119–123.
29. **Wang L, Jeng KS, Lai MM.** 2011. Poly(C)-binding protein 2 interacts with sequences required for viral replication in the hepatitis C virus (HCV) 5′ untranslated region and directs HCV RNA replication through circularizing the viral genome. J. Virol. **85**:7954–7964.
30. **Yi M, Villanueva RA, Thomas DL, Wakita T, Lemon SM.** 2006. Production of infectious genotype 1a hepatitis C virus (Hutchinson strain) in cultured human hepatoma cells. Proc. Natl. Acad. Sci. U. S. A. **103**:2310–2315.

Stabilization of hepatitis C virus RNA by an Ago2–miR-122 complex

Tetsuro Shimakami[a,1], Daisuke Yamane[a,1], Rohit K. Jangra[a,1,2], Brian J. Kempf[b], Carolyn Spaniel[a], David J. Barton[b], and Stanley M. Lemon[a,3]

[a]Lineberger Comprehensive Cancer Center and Division of Infectious Diseases, Department of Medicine, University of North Carolina at Chapel Hill, Chapel Hill, NC 27599-7292; and [b]Department of Microbiology, University of Colorado School of Medicine, Aurora, CO 80045

Edited* by Charles M. Rice, The Rockefeller University, New York, NY, and approved December 5, 2011 (received for review July 27, 2011)

MicroRNAs (miRNAs) are small noncoding RNAs that regulate eukaryotic gene expression by binding to regions of imperfect complementarity in mRNAs, typically in the 3′ UTR, recruiting an Argonaute (Ago) protein complex that usually results in translational repression or destabilization of the target RNA. The translation and decay of mRNAs are closely linked, competing processes, and whether the miRNA-induced silencing complex (RISC) acts primarily to reduce translation or stability of the mRNA remains controversial. miR-122 is an abundant, liver-specific miRNA that is an unusual host factor for hepatitis C virus (HCV), an important cause of liver disease in humans. Prior studies show that it binds the 5′ UTR of the messenger-sense HCV RNA genome, stimulating translation and promoting genome replication by an unknown mechanism. Here we show that miR-122 binds HCV RNA in association with Ago2 and that this slows decay of the viral genome in infected cells. The stabilizing action of miR-122 does not require the viral RNA to be translationally active nor engaged in replication, and can be functionally substituted by a nonmethylated 5′ cap. Our data demonstrate that a RISC-like complex mediates the stability of HCV RNA and suggest that Ago2 and miR-122 act coordinately to protect the viral genome from 5′ exonuclease activity of the host mRNA decay machinery. miR-122 thus acts in an unconventional fashion to stabilize HCV RNA and slow its decay, expanding the repertoire of mechanisms by which miRNAs modulate gene expression.

RNA decay | viral host factor

MicroRNAs (miRNAs) typically regulate eukaryotic gene expression by binding to regions of imperfect complementarity in the 3′ UTR of mRNAs, recruiting an Argonaute (Ago) protein complex that results in translational repression or destabilization of the target RNA (1). Although miRNAs regulate a majority of genes, an unresolved question is whether the miRNA-induced silencing complex (RISC) acts primarily to reduce translation or enhance decay of the mRNA, two closely linked, competing processes (2–4). miR-122 is an abundant, liver-specific miRNA, comprising >50% of mature miRNAs in human hepatocytes and regulating the expression of numerous hepatic genes, including those involved in fatty acid and cholesterol metabolism (5, 6). It is also a very unusual host factor required for replication of hepatitis C virus (HCV), an important cause of liver disease in humans (7, 8). Prior studies show that miR-122 binds the 5′ UTR of the positive-strand HCV RNA genome (7, 9), stimulating viral protein expression and promoting viral replication by a poorly understood mechanism (10, 11).

Although miR-122 does not directly stimulate HCV RNA synthesis (12, 13), its ability to promote genome amplification is independent of its regulation of hepatic metabolism (12) and requires the binding of its "seed sequence" (nucleotides 2–8) to two conserved sites (S1 and S2) in the viral 5′ UTR (7, 9). Additional "supplementary" base-pairing between miR-122 and HCV RNA sequences upstream of S1 and S2 has also been recognized recently and shown to be essential for promotion of genome amplification (14, 15). The miR-122 binding sites are near the 5′ end of the RNA and immediately upstream of an internal ribosome entry site (IRES) that has high affinity for the 40S ribosome subunit (16). The unusual ability of miR-122 to stimulate viral protein translation (10, 11) is dependent on where it binds, because miR-122 suppresses expression of capped reporter mRNAs that contain the HCV target sequence in the 3′ UTR (9). Translation enhancement only partially explains the role of miR-122 in the HCV life cycle, however, because mutant viral RNAs that are deficient in miR-122 binding are far more handicapped in their ability to replicate than viral RNAs with mutations in the IRES that result in quantitatively comparable defects in translation (11).

Although there has been speculation that miR-122 might promote genome amplification and viral protein expression by physically stabilizing HCV RNA (14, 17), previous experimental results suggest this is not the case and that miR-122 does not enhance RNA stability (7, 10). Here we present a contrasting view and show that binding of miR-122 to the 5′ terminus of HCV RNA in association with Ago2 significantly slows decay of the viral RNA genome in infected cells. miR-122 thus acts in an unconventional fashion to stabilize HCV RNA, expanding the repertoire of mechanisms by which miRNAs modulate gene expression.

Results

We studied how miR-122 influences the stability of synthetic HCV RNA transfected into human hepatoma cells. Northern blots demonstrated significant increases in the abundance of a replication-defective viral RNA (H77S/GLuc2A-AAG, that contains a lethal mutation in its RNA polymerase) (Fig. 1*A*) when it was electroporated into cells together with duplex miR-122 (Fig. 1*B*). miR-124, a brain-specific miRNA that does not bind HCV RNA, had no such effect. Conversely, cotransfection of viral RNA with 2′O-methyl-modified (2′OMe) or locked nucleic acid antisense oligoribonucleotides capable of sequestering miR-122 reduced the abundance of HCV RNA at 3, 6, and 9 h after electroporation. These differences were reproducible in multiple experiments and observed with HCV RNAs containing 5′ UTR sequence from either genotype 1 (H77) or genotype 2 (JFH1) virus. We estimated the rate of viral RNA decay by PhosphorImager analysis of Northern blots, normalizing HCV RNA abundance (HCV RNA/actin mRNA) to that present at 3 h after electroporation to compare rates of

Author contributions: T.S., D.Y., R.K.J., B.J.K., C.S., D.J.B., and S.M.L. designed research; T.S., D.Y., R.K.J., C.S., and B.J.K. performed research; T.S., D.Y., R.K.J., B.J.K., C.S., D.J.B., and S.M.L. analyzed data; and T.S., D.Y., R.K.J., D.J.B., and S.M.L. wrote the paper.

The authors declare no conflict of interest.

*This Direct Submission article had a prearranged editor.

[1]T.S., D.Y., and R.K.J. contributed equally to this work.

[2]Present address: Department of Microbiology, Mount Sinai School of Medicine, New York, NY 10029.

[3]To whom correspondence should be addressed. E-mail: smlemon@med.unc.edu.

This article contains supporting information online at www.pnas.org/lookup/suppl/doi:10.1073/pnas.1112263109/-/DCSupplemental.

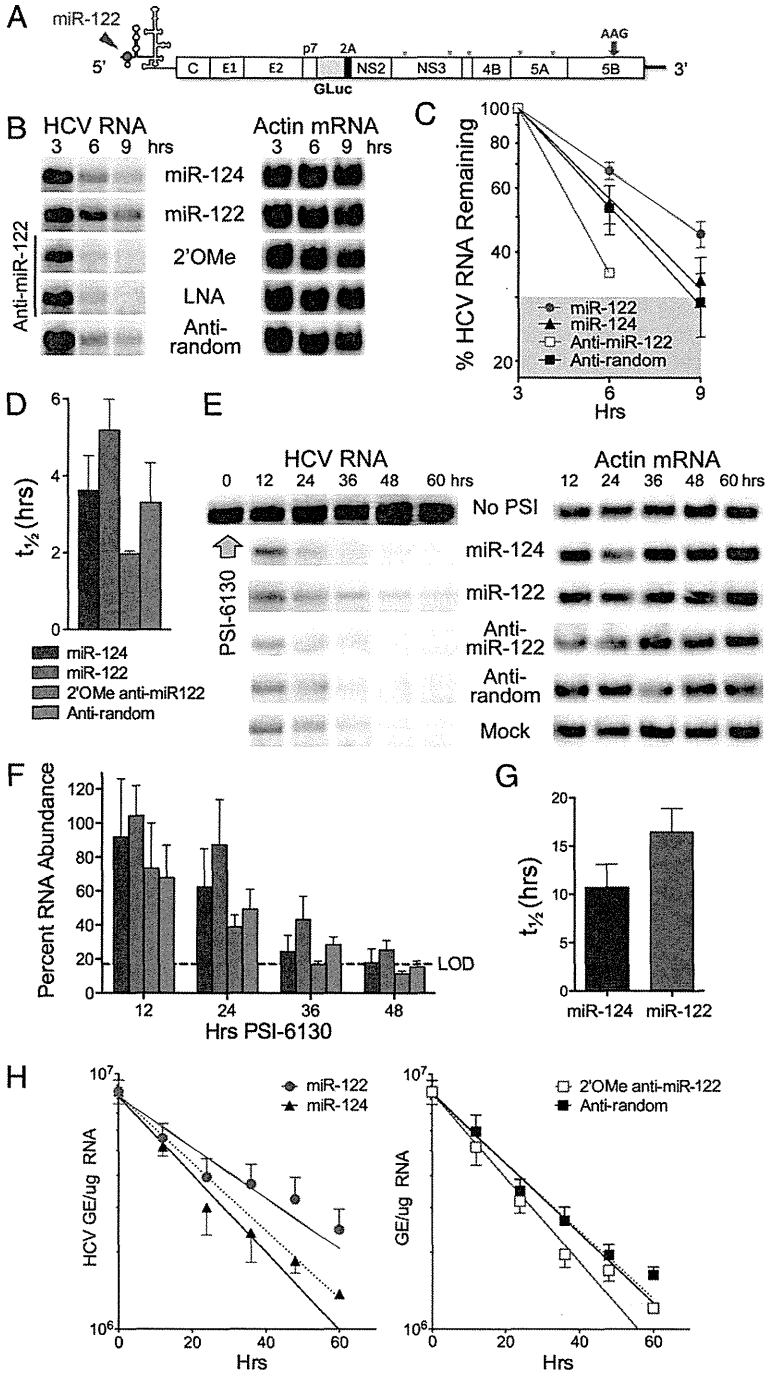

Fig. 1. miR-122 stabilizes the HCV RNA genome. (*A*) Organization of H77S/GLuc2A-AAG RNA that expresses GLuc as part of the HCV polyprotein (31). The AAG mutation in NS5B ablates genome amplification. The position at which miR-122 binds the 5′ UTR is shown. (*B*) Northern blot of H77S/GLuc2A-AAG and actin RNA (loading control) in Huh-7.5 cells after electroporation of viral RNA together with duplex miRNAs or antisense oligoribonucleotides. (*C*) Quantitation of HCV RNA relative to actin mRNA by phosphorimaging of Northern blots from five independent electroporation experiments. Data shown represent the mean percentage RNA remaining (±SEM) relative to that present at 3 h after electroporation under each condition. Data were fit to a one-phase decay model (R^2 = 0.87–0.99). The shaded area represents the approximate limit of detection (LOD; 9 h posttransfection data from anti-miR-122–transfected cells were below the LOD and excluded from analysis). (*D*) Mean HCV RNA $t_{1/2}$ estimated by fitting the Northern blot data to a one-phase decay model, as shown in *C*. Error bars indicate 95% confidence intervals. (*E*) Northern blot of HCV RNA in persistently infected (>3 wk) cells treated with PSI-6130 (10 μM or >10-fold the EC_{50}) and transfected with miRNAs or 2′OMe oligoribonucleotides. (*F*) PhosphorImager quantitation of Northern blots in two replicate experiments involving PSI-6130 treatment. Results were normalized to RNA abundance in mock-transfected cells at 12 h. See *D* for the key. (*G*) Mean HCV RNA $t_{1/2}$ ± SD in cells supplemented with miR-122 vs. miR-124 after PSI-6130 treatment, estimated by fitting PhosphorImager data from four independent experiments to a one-phase decay model. P = 0.007 by two-sided paired t test. (*H*) qRT-PCR determination of HCV RNA decay in infected cells treated with PSI-6130 and supplemented with miRNAs and antisense oligoribonucleotides as in *E*. Data are from three replicate infected cultures, and represent HCV genome equivalents (GE) per μg total RNA ± SD (*left*) HCV RNA in cells supplemented with miR-122 or miR-124. Data were fit to a one-phase decay model (R^2 = 0.86–0.95): HCV RNA $t_{1/2}$ =30.3 h for miR-122 vs. 19.8 h for miR-124 (P = 0.018). *Right*: Cells treated with 2′-OMe anti-miR-122 or anti-random (R^2 = 0.95–0.96): $t_{1/2}$ =18.2 h for anti-miR-122 vs. 21.9 h for anti-random (P = 0.023). The dashed line in both panels represents the one-phase decay curve in mock-treated cells.

decay between 3 and 9 h under different conditions (Fig. 1*C*). This allowed for recovery of the cells after electroporation, and when the data were fit to a one-phase decay model, indicated that the half-life ($t_{1/2}$) of HCV RNA in cells cotransfected with miR-122 was 5.2 h vs. 3.60 h for cells cotransfected with miR-124 ($P = 0.0035$ by the extra sum-of-squares F test) and 3.3 vs. 2.0 h for cells transfected with anti-random vs. the anti–miR-122 antagomir ($P = 0.0016$) (Fig. 1*D*). Similar differences in rates of decay were observed when HCV RNA was assayed by quantitative RT-PCR (qRT-PCR) (Fig. S1*A*). Differences in RNA decay were matched by differences in viral protein expression (Fig. S1*B*), monitored by measuring *Gaussia* luciferase (GLuc) encoded by sequence inserted into the viral genome (Fig. 1*A*). Taken together, these results indicate that miR-122 positively regulates the stability of transfected HCV RNA. The corresponding increase in protein expression provides a logical explanation for the enhanced HCV translation reported previously (10, 11).

Because transfected RNA is likely to be subject to different decay pathways than replicating viral genomes in infected cells, we determined whether miR-122 also slows degradation of viral RNA in infected cells treated with PSI-6130, a potent and specific nucleoside inhibitor that arrests new viral RNA synthesis (18). Under these conditions, as expected, viral RNA degraded more slowly than after electroporation (compare Fig. 1 *B* and *E*). However, its rate of decay was reduced when miR-122 was transfected simultaneously with PSI-6130 treatment (Fig. 1*E*). When fit to a one-phase decay model, PhosphorImager data from replicate experiments (Fig. 1*F*) indicated a significant difference in the rate constant for HCV RNA decay, k ($k = \ln(2)/t_{1/2}$), in cells supplemented with miR-122 vs. miR-124 ($P = 0.048$ by the extra sum-of-squares F test). The difference in the $t_{1/2}$ was highly significant statistically ($P = 0.007$ by two-sided paired t test) (Fig. 1*G*). Likewise, increases in the decay rate in cells transfected with anti-miR-122 vs. the control anti-random oligonucleotide were also significant ($P = 0.014$ by F test), whereas decay rate constants were similar in cells receiving anti-miR-124, anti-random, or mock treatment ($P > 0.05$). Similar results were observed when miR-122 was transfected into cells 8 h after the addition of PSI-6130, which would allow for any potential delay in suppression of viral RNA synthesis due to the need for phosphorylation of the inhibitor (Fig. S1 *C* and *D*).

In a completely independent set of experiments, we used qRT-PCR to quantify HCV RNA in infected cells treated with PSI-6310. The results suggested a longer $t_{1/2}$ for HCV RNA (≈19 h vs. ≈10 h) in miR-124–treated cells than that determined by Northern analysis. This is likely to reflect the small size of the RNA segment detected in the RT-PCR assay (221 bases vs. the 9.7-kb RNA genome detected in Northern blots) and the inability of the RT-PCR assay to discriminate between intact and partially degraded RNAs. However, we again observed significant differences in HCV RNA decay rates in cells supplemented with miR-122 vs. miR-124, or anti-miR-122 vs. anti-random (Fig. 1*H*). Although the magnitude of this effect is relatively small (not unlike the impact of miRNAs on cellular mRNA translation), these data show collectively that miR-122 reproducibly stabilizes the viral RNA genome in infected cells.

We next determined whether miR-122 could directly stabilize RNA in a cell-free system. For this, we compared poliovirus (PV) RNA and a related RNA (DNVR2) in which the PV 5′ UTR was replaced with the HCV 5′ UTR (Fig. 2*A*). The stabilities of these RNAs have been compared previously in S10 translation mixtures prepared from HeLa cells (19, 20), providing a useful context for these experiments. PV RNA is stabilized in these extracts by poly(rC) binding protein 1 (hnRNP1-E1), which associates with a 5′-terminal cloverleaf RNA structure, and decays more slowly than DNVR2 RNA (20). However, DNVR2 RNA stability was increased and approximated that of PV RNA when duplex miR-122, but not miR-124, was added to S10 reactions before the viral RNA (Fig. 2 *B* and *C*). The stabilization of DNVR2 RNA by miR-122 was reproducible and statistically significant (Fig. 2 legend). In contrast, neither miRNA enhanced stability of PV RNA lacking HCV sequence. Thus, miR-122 directly regulates stability of RNA containing the HCV 5′ UTR and does not accomplish this indirectly by modulating cellular gene expression.

Mutations in S1 and S2 that ablate miR-122 binding are lethal to replication of HCV that has been adapted to growth in cell culture (HJ3-5 virus) (11). Similarly, Northern blots revealed that an HCV mutant defective in miR-122 binding at both sites (S1-S2-p6m; Fig. 3*A*) (11), as well as polymerase function (GDD to GND substitution in NS5B), was not stabilized by miR-122 when transfected into hepatoma cells (Fig. 3*B*, compare lanes 1–3 vs. 4–6). In contrast, the complementary miR-122 mutant (miR-122p6) (Fig. 3*A*) did stabilize S1-S2-p6m RNA (Fig. 3*B*, lanes 1–3 vs. 7–9) but not viral RNA with WT S1 and S2 sequences. The differences in HCV RNA abundance apparent in these blots were reproduced in multiple experiments, statistically significant (Fig. S2*A*), and mirrored by differences in GLuc expressed from these nonreplicating viral RNAs (Fig. S2*B*). Collectively, these data indicate that HCV RNA is physically stabilized as a result of miR-122 binding to its 5′ UTR, a unique action for a miRNA.

Because mRNA translation and decay are closely coupled processes (2), we considered the possibility that miR-122 could stabilize the RNA by promoting its translation. We thus evaluated its ability to slow decay of an RNA containing three consecutive base substitutions in an RNA loop within the HCV IRES [mutant G(266-8)C; Fig. 3*C*]. These base changes eliminate IRES affinity for the 40S ribosome particle and ablate translation (11, 16), even in cells supplemented with miR-122 (Fig. S3*A*). Consistent with the notion that translation and decay are intrinsically linked (2), Northern blots of cells transfected with equivalent amounts of WT and G(266-8)C RNA (both containing an NS5B mutation ablating RNA replication) consistently showed a lower abundance of the G(266-8)C mutant, suggesting that it was less stable than RNA with a WT 5′ UTR (Fig. 3 *D* and *E*). Nonetheless, decay of the translationally

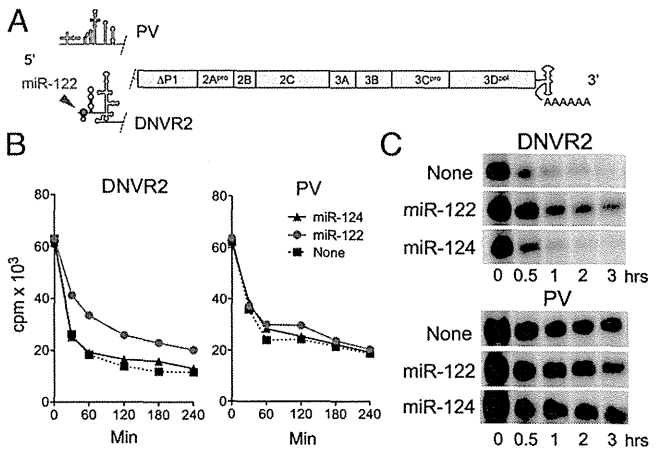

Fig. 2. miR-122 stabilizes synthetic RNA containing the HCV 5′ UTR. (*A*) Structure of DNVR2 and PV RNAs (19), which differ only in 5′ UTR sequence. (*B*) miR-122 slows decay of DNVR2 RNA in HeLa S10 lysate. Data shown represent acid-precipitable α-[^{32}P]-CTP-labeled RNA in HeLa S10 reaction mixtures (19) containing 1 μM of duplex miRNA. The DNVR2 decay constant in miR-122– vs. miR-124–supplemented mixtures, estimated by fitting the data to a one-phase decay model ($R^2 = 0.972$–0.989), differed significantly ($P = 0.002$). (*C*) RNA extracted from HeLa S10 reaction mixtures and fractionated by electrophoresis in 0.8% agarose.

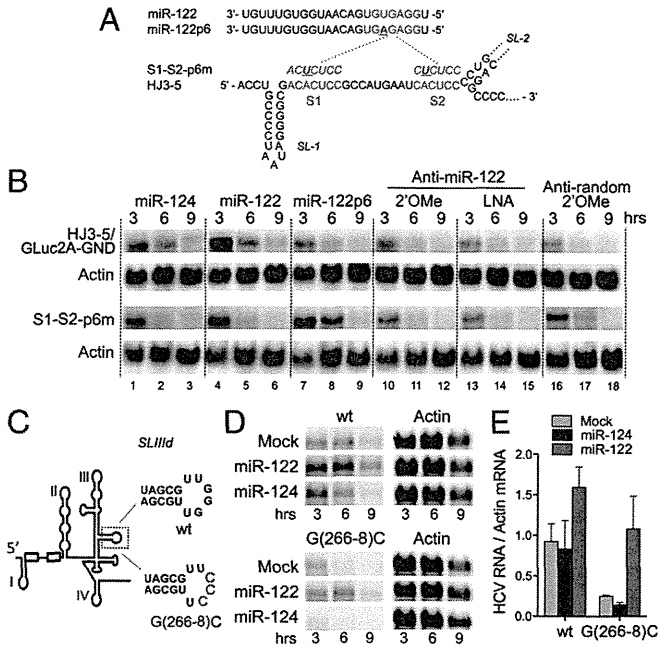

Fig. 3. Stabilization of HCV RNA requires miR-122 binding and is independent of translation. (*A*) *Upper*: miR-122 and mutant miR-122p6 guide-strand sequences. *Lower*: 5′ terminal sequence of HCV (HJ3-5/GLuc2A virus), with S1 and S2 binding sites shown in red. Point mutations (underlined) in the related S1-S2-p6m-GND mutant (11) are shown above. SL-1 and SL-2 are putative stem-loop structures in the 5′ UTR. (*B*) Northern blots of HJ3-5/GLuc2A-GND and the related S1-S2-p6m-GND mutant RNA after transfection into Huh-7.5 cells with RNA oligoribonucleotides as in Fig. 1*B*. (*C*) Putative secondary structure of the HCV 5′ UTR, showing the location of stem-loop IIId and the G(266-8)C IRES mutation that ablates translation. (*D*) Northern blot showing HCV RNA abundance in MEFs transfected with HCV RNA (H77S/GLuc2A-AAG) containing (*Upper*) the WT 5′ UTR vs. (*Lower*) the translationally inactive G(266-8)C mutant, and supplemented with the indicated miRNAs. (*E*) PhosphorImager quantitation of HCV RNA in Northern blots of 6-h cell lysates from two independent experiments carried out as shown in *D*.

inactive mutant was significantly slowed when the cells were supplemented with miR-122 (Fig. 3 *D* and *E*). These experiments were carried out in murine embryonic fibroblasts (MEFs) that do not express detectable endogenous miR-122. Similar results were obtained both in MEFs and hepatoma cells with another IRES mutant, G(267)C, that retains affinity for the 40S subunit but is also translationally dead (11, 16) (Fig. S3 *B*–*E*). Collectively these results show that miR-122 does not stabilize HCV RNA by promoting its translation or enhancing its association with ribosomes. Active engagement in translation and miR-122 promote stability of the RNA genome independently, and possibly additively.

Randall et al. (21) reported previously that RNAi-mediated depletion of any of the Ago proteins (particularly Ago4) or Dicer inhibited the ability of HCV to infect cells. In contrast, we found that only Ago2 depletion (Fig. S4*A*) inhibited HCV RNA replication in hepatoma cells with previously established infection (Fig. 4*A*). Ago2 depletion had no effect on cell growth (Fig. S4*B*) but reduced both HCV RNA abundance and protein expression (Fig. 4*A*). This was not observed with depletion of other Ago proteins or Dicer. Although we are uncertain why our results differ from those of Randall et al. (21), they suggest that Ago2 plays a special role in HCV replication. Two recent studies are consistent with this: they show Ago2 to be required for miR-122 to promote HCV genome amplification (15, 22). However, a third study found no impairment in miR-122 modulation of HCV in Ago2-depleted cells (14).

Consistent with the stabilization of HCV RNA requiring interaction with an miR-122–associated RISC complex, we observed no stabilizing or translation-enhancing effect in hepatoma cells transfected with single-stranded miR-122 (guide strand only, rather than the duplex miRNA transfected in previous experiments) (Fig. S4*C*). To determine whether miR-122 binds as a complex with Ago2, we lysed MEFs shortly after electroporation with HCV RNA together with duplex miR-122 and used RT-PCR to interrogate Ago2 immunoprecipitates for the presence of viral RNA. HCV RNA with WT S1 and S2 sequence coimmunoprecipitated with Ago2 (Fig. 4*B*). However, RNA with point mutations in S1 and S2 that ablate miR-122 binding (Fig. 3*A*) coimmunoprecipitated with Ago2 only when cells were supplemented with the complementary miR-122 mutant, miR-122p6 (Fig. 4*B*). Transfected HCV RNA was also enriched in anti-Flag immunoprecipitates from hepatoma cells ectopically expressing Flag-Ago2 vs. Flag-Ago1 (Fig. S5). Thus, miR-122 binds the HCV 5′ UTR in association with Ago2. Lesser amounts of Ago1 may also be present in the complex.

To determine whether Ago2 plays a functional role in stabilizing HCV RNA, we compared the ability of miR-122 to slow the decay of the RNA when electroporated with it into WT or Ago2-deficient ($Ago2^{-/-}$) MEFs (23). This revealed a striking dependence on Ago2, because miR-122 had no effect in $Ago2^{-/-}$ MEFs, whereas it significantly stabilized the viral RNA and enhanced viral translation in matched WT cells (Fig. 4 *C* and *D*). Ectopic expression of human Flag-Ago2 in the $Ago2^{-/-}$ MEFs restored the ability of miR-122 to positively regulate protein expression from HCV RNA, further confirming the requirement for Ago2 (Fig. S6). To ascertain whether it is possible for other Ago proteins to functionally substitute for Ago2 in stabilizing HCV RNA, we also overexpressed human Flag-Ago1 in the $Ago2^{-/-}$ MEFs. This only partially rescued the ability of miR-122 to promote HCV protein expression (Fig. S6*B*), although immunoblots with anti-Flag antibody indicated that Flag-Ago1 was overexpressed at almost threefold the abundance of Flag-Ago2 and well above physiologically relevant levels (Fig. S6*A*). Thus, Ago2 is not unique in its ability to support miR-122 enhancement of HCV protein expression, but it seems to do this more efficiently than Ago1. This is consistent with the greater enrichment of HCV RNA we observed in Flag-Ago2 compared with Flag-Ago1 immunoprecipitates (Fig. S5). Additional experiments confirmed that Ago2 is the dominant Ago protein involved in miR-122 stabilization of HCV RNA. RNAi-mediated depletion of Ago2 reduced the ability of miR-122 to stabilize HCV RNA and promote its translation in HeLa cells (Fig. S7 *A*–*D*). Importantly, the magnitude of this effect mirrored the reduction in miR-122–mediated suppression of a reporter mRNA containing the HCV miR-122 binding sites within its 3′ UTR (9) (Fig. S7*E*).

These results suggest a functional interaction of Ago2 with RNA decay machinery. Because HCV RNA lacks a 5′ m^7G cap, one possibility is that miR-122 recruits an Ago2 RISC complex to the 5′ end of viral RNA that protects it from 5′ exonuclease activity. If so, this protective action should be rendered redundant by providing the RNA with a 5′ cap. To test this, we synthesized HCV RNAs with or without a 5′ nonmethylated guanosine cap analog and compared their stabilities after transfection into MEFs with or without miR-122. As anticipated, miR-122 had no effect on the rate of decay of the 5′ capped RNA, whereas it substantially stabilized the uncapped HCV RNA (Fig. 5*A*). The magnitude of protein expression (GLuc) from capped RNA was comparable to that from the uncapped RNA in cells supplemented with miR-122 and was not further increased by miR-122 (Fig. 5*B*). Thus, the 5′ cap enhanced stability and protein expression from HCV RNA, functionally substituting for miR-122 and providing strong evidence that the miR-122–Ago2 complex protects HCV RNA from 5′ exonuclease. Importantly,

translation of the capped HCV RNA was IRES-dependent, because the nonmethylated 5′ cap lacked the ability to recruit eukaryotic initiation factors.

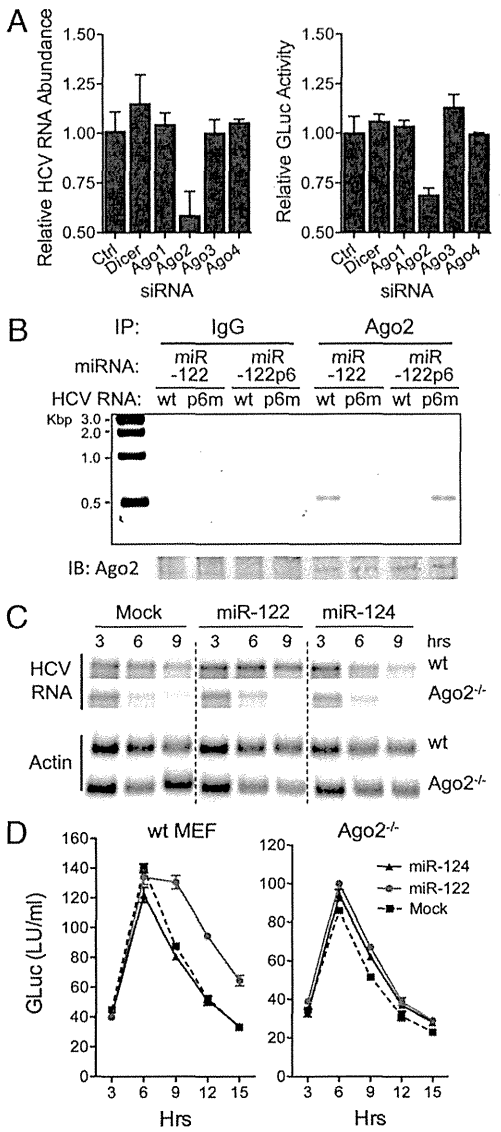

Fig. 4. Ago2 binds HCV RNA in association with miR-122 and is required for stabilization. (*A*) RNAi depletion of Ago2 impairs HCV genome amplification in persistently infected (HJ3-5/GLuc2A virus) cells. *Left*: HCV RNA abundance relative to that in cells transfected with nontargeting siRNA (Ctrl) 72 h after siRNA transfection. RNA was assayed by qRT-PCR; data are mean ± range of paired cultures. *Right*: GLuc activity secreted into media between 48 and 72 h, relative to si-Ctrl-transfected cultures (mean ± range). (*B*) miR-122 binds HCV RNA as a complex with Ago2. Lysates were prepared from WT MEFs 6 h after electroporation with HJ3-5/GND or S1-S2-p6m-GND RNA (Fig. 3*A*), mixed with miR-122 or miR-122p6, and immunoprecipitated with anti-Ago2 antibody. After extensive washing, RNA was extracted from the precipitates and subjected to a one-step HCV-specific RT-PCR (30 cycles). HCV RNA was enriched in precipitates from HJ3-5/GND–transfected cells supplemented with miR-122, or S1-S2-p6m-GND cells supplemented with miR-122p6. (*C*) Northern blots showing miR-122 does not stabilize HCV RNA in Ago2$^{-/-}$ MEFs. Cells were electroporated with HCV RNA (H77S/GLuc2A-AAG) together with miR-122, miR-124, or no miRNA (Mock), then lysed at 3-h intervals and assayed for HCV RNA abundance. miR-122 stabilized HCV RNA only in WT MEFs and was without effect in Ago2$^{-/-}$ cells. (*D*) GLuc activity in supernatant fluids from MEFs cotransfected with HCV RNA and the indicated miRNA (mean ± range). Data shown are representative of two or more independent experiments.

Discussion

Our results reveal a unique mechanism by which a miRNA in association with Ago2 regulates the expression of its target RNA, in this case the HCV genome. Although miR-10a enhances translation by binding the 5′ UTR of ribosomal protein mRNAs containing 5′ terminal oligopyrimidine (TOP) motifs (24), miRNAs have not been recognized to slow decay or up-regulate abundance of their RNA targets. miR-122 does this by recruiting an Ago2 RISC-like complex to the 5′ end of the HCV RNA genome. As evidenced by the IRES mutants (Fig. 3*D* and Fig. S3*D*), the stabilizing action of miR-122 does not require the target HCV RNA to be capable of translation and thus does not result from increased ribosomal loading. Stabilization also does not require the RNA to be replication competent (Fig. 1 *B* and *C*).

Because a nonmethylated 5′ cap analog functionally substitutes for miR-122 (Fig. 5), the RISC-like complex recruited by miR-122 is likely to act by protecting the RNA from 5′ exonuclease. Whether this occurs simply as a result of physically masking the 5′ end of the viral RNA from 5′ exonuclease attack, or whether Ago2 plays a more complex role by influencing the association of HCV RNA with P bodies (25), sites of mRNA degradation and storage, remains to be determined. Binding of a RISC-like complex could also limit recognition of the 5′ triphosphate of HCV RNA by retinoic acid-inducible gene I (RIG-I), a ubiquitous innate immune pathogen recognition receptor (26) that is capable of inducing interferons and interferon-stimulated genes, including RNase L, an endonuclease, and ISG20, a 3′-5′ exonuclease (27). However, subversion of RIG-I–dependent viral RNA degradation played no role in the stabilization of HCV RNA in our experiments because the Huh-7.5 cells used are deficient in RIG-I signaling (28).

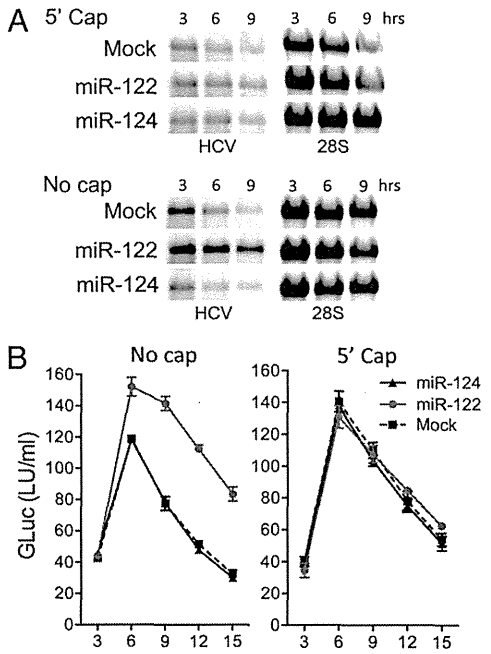

Fig. 5. A nonmethylated 5′ guanosine cap functionally substitutes for miR-122 in stabilizing HCV RNA. (*A*) Northern blots of HCV RNA in lysates of MEFs after electroporation with HCV RNA (H77S/GLuc2A-AAG) (Fig. 1*A*) synthesized with or without a nonmethlyated G[5′]ppp[5′]G-RNA cap. HCV RNAs were transfected together with miR-122, miR-124, or no miRNA (Mock). 28S rRNA is shown as a loading control. (*B*) GLuc activity in supernatant fluids of MEFs transfected with capped or uncapped HCV RNAs (mean ± range of two replicate cultures). Data shown are representative of two or more independent experiments.

The mechanism by which miR-122 stabilizes HCV RNA is distinct from the up-regulation of translation by miRNAs that target AU-rich elements within the 3′ UTRs of some mRNAs, because the latter occurs only in quiescent cells arrested at the G_0 phase of the cell cycle (29, 30). Moreover, miRNA-mediated stimulation of translation in quiescent cells has not been linked to stabilization of the target mRNA, as we show here for miR-122. Still to be determined is whether the protein composition of the RISC-like complex that is recruited to the 5′ UTR by miR-122 differs significantly from miRNA-induced RISC complexes involved in translational repression.

The stabilization of HCV RNA by miR-122 is likely to be responsible for the miR-122–induced enhancement of HCV translation reported previously (10, 11). Mutations in the viral RNA that prevent binding of miR-122 also ablate replication of infectious virus (11) and prevent stabilization of the genome by miR-122 (Fig. 3). Depletion of Ago2 has similar effects on replication, translation, and RNA stability (15, 22) (Fig. 4). This makes it difficult to distinguish between these consequences of miR-122 binding to the 5′ UTR or to determine the primary role played by miR-122 as a host factor for viral replication. However, stabilization of the genome is likely to be a key factor in the promotion of viral replication by miR-122. A recombinant HCV in which the U3 RNA sequence was inserted in lieu of the S1 binding site in the 5′ UTR was found recently to be less dependent upon miR-122 for replication (17), possibly because the U3 sequence stabilized the RNA, much as a 5′ cap did (Fig. 5). Nonetheless, it would not be surprising to find that miR-122 has other functions in the viral life cycle in addition to its role in stabilizing the viral RNA genome, perhaps in the initiation of viral RNA synthesis.

Methods

Viral RNA Stability in Transfected Cells. RNA was transcribed in vitro (11) from pH77S/GLuc2A-AAG, which contains the complete genotype 1a HCV sequence with GLuc2A placed in-frame within the polyprotein-coding region (31) and a lethal GDD to AAG mutation in NS5B. Where indicated, a non-methylated 5′ guanosine cap was added using the ScriptCap m7G Capping System (Epicentre Biotechnologies). Viral RNA (20 μg) and miRNA duplexes (11) or antisense oligoribonucleotides (1 μM) were mixed with 1×10^7 Huh-7.5 cells in a 4-mm cuvettete and pulsed once at 250 V, 950 μF, and 100 Ω in a Gene Pulser Xcell Total System (Bio-Rad). HeLa cells were electroporated at 300 V, 500 μF, and ∞ Ω, and MEFs at 400 V, 250 μF, and ∞ Ω. Cells were harvested at intervals and supernatant fluids assayed for GLuc activity (31) and HCV RNA abundance in cell lysates assessed by Northern blotting (11). Polyadenylated reporter RNAs encoding firefly or *Cypridina* luciferase were cotransfected to monitor transfection efficiency (11).

HCV-Infected Cells. Synthetic HJ3-5 or HJ3-5/GLuc2A RNA (31) was transfected into 1×10^7 FT3-7 cells, which were passaged until >90% positive for core antigen in an immunofluorescence assay (11). siRNA pools targeting Ago1-4 or Dicer and control siRNA pools (Dharmacon) were transfected using siLentfect Lipid Reagent (Bio-Rad). miRNA duplexes or single-stranded oligoribonucleotides (50 nM) were transfected using Lipofectamine 2000 (Invitrogen).

Additional methods and associated references can be found in *SI Methods*.

ACKNOWLEDGMENTS. We thank Lucinda Hensley for expert technical assistance; William F. Marzluff and Scott M. Hammond for helpful discussions; Alexander Tarakhovsky and Angela Santana, Rockefeller University, for mouse embryonic fibroblasts; Charles Rice, Rockefeller University, for Huh-7.5 cells; Thorleif Møller, Mirrx Therapeutics, for psi-Check2/Luc-3′ HCV DNA; and Angela Lam and Phil Furman, Pharmasset, Inc., for PSI-6130. This study was supported in part by the University Cancer Research Fund and National Institutes of Health Grants RO1-AI095690, U19-AI040035, P20-CA150343 (to S.M.L.), and AI042189 (to D.J.B.). R.K.J. was supported by a James W. McLaughlin Fellowship.

1. Fabian MR, Sonenberg N, Filipowicz W (2010) Regulation of mRNA translation and stability by microRNAs. *Annu Rev Biochem* 79:351–379.
2. Balagopal V, Parker R (2009) Polysomes, P bodies and stress granules: States and fates of eukaryotic mRNAs. *Curr Opin Cell Biol* 21:403–408.
3. Djuranovic S, Nahvi A, Green R (2011) A parsimonious model for gene regulation by miRNAs. *Science* 331:550–553.
4. Guo H, Ingolia NT, Weissman JS, Bartel DP (2010) Mammalian microRNAs predominantly act to decrease target mRNA levels. *Nature* 466:835–840.
5. Chang J, et al. (2004) miR-122, a mammalian liver-specific microRNA, is processed from hcr mRNA and may downregulate the high affinity cationic amino acid transporter CAT-1. *RNA Biol* 1:106–113.
6. Lanford RE, et al. (2010) Therapeutic silencing of microRNA-122 in primates with chronic hepatitis C virus infection. *Science* 327:198–201.
7. Jopling CL, Yi M, Lancaster AM, Lemon SM, Sarnow P (2005) Modulation of hepatitis C virus RNA abundance by a liver-specific MicroRNA. *Science* 309:1577–1581.
8. Chisari FV (2005) Unscrambling hepatitis C virus-host interactions. *Nature* 436: 930–932.
9. Jopling CL, Schütz S, Sarnow P (2008) Position-dependent function for a tandem microRNA miR-122-binding site located in the hepatitis C virus RNA genome. *Cell Host Microbe* 4:77–85.
10. Henke JI, et al. (2008) microRNA-122 stimulates translation of hepatitis C virus RNA. *EMBO J* 27:3300–3310.
11. Jangra RK, Yi M, Lemon SM (2010) miR-122 regulation of hepatitis C virus translation and infectious virus production. *J Virol* 84:6615–6625.
12. Norman KL, Sarnow P (2010) Modulation of hepatitis C virus RNA abundance and the isoprenoid biosynthesis pathway by microRNA miR-122 involves distinct mechanisms. *J Virol* 84:666–670.
13. Villanueva RA, et al. (2010) miR-122 does not modulate the elongation phase of hepatitis C virus RNA synthesis in isolated replicase complexes. *Antiviral Res* 88: 119–123.
14. Machlin ES, Sarnow P, Sagan SM (2011) Masking the 5′ terminal nucleotides of the hepatitis C virus genome by an unconventional microRNA-target RNA complex. *Proc Natl Acad Sci USA* 108:3193–3198.
15. Roberts AP, Lewis AP, Jopling CL (2011) miR-122 activates hepatitis C virus translation by a specialized mechanism requiring particular RNA components. *Nucleic Acids Res* 39:7716–7729.
16. Kieft JS, Zhou K, Jubin R, Doudna JA (2001) Mechanism of ribosome recruitment by hepatitis C IRES RNA. *RNA* 7:194–206.
17. Li YP, Gottwein JM, Scheel TK, Jensen TB, Bukh J (2011) MicroRNA-122 antagonism against hepatitis C virus genotypes 1-6 and reduced efficacy by host RNA insertion or mutations in the HCV 5′ UTR. *Proc Natl Acad Sci USA* 108:4991–4996.
18. Ma H, et al. (2007) Characterization of the metabolic activation of hepatitis C virus nucleoside inhibitor beta-D-2′-Deoxy-2′-fluoro-2′-C-methylcytidine (PSI-6130) and identification of a novel active 5′-triphosphate species. *J Biol Chem* 282:29812–29820.
19. Lyons T, Murray KE, Roberts AW, Barton DJ (2001) Poliovirus 5′-terminal cloverleaf RNA is required in cis for VPg uridylylation and the initiation of negative-strand RNA synthesis. *J Virol* 75:10696–10708.
20. Murray KE, Roberts AW, Barton DJ (2001) Poly(rC) binding proteins mediate poliovirus mRNA stability. *RNA* 7:1126–1141.
21. Randall G, et al. (2007) Cellular cofactors affecting hepatitis C virus infection and replication. *Proc Natl Acad Sci USA* 104:12884–12889.
22. Wilson JA, Zhang C, Huys A, Richardson CD (2011) Human Ago2 is required for efficient miR-122 regulation of HCV RNA accumulation and translation. *J Virol* 85: 2342–2350.
23. O'Carroll D, et al. (2007) A Slicer-independent role for Argonaute 2 in hematopoiesis and the microRNA pathway. *Genes Dev* 21:1999–2004.
24. Ørom UA, Nielsen FC, Lund AH (2008) MicroRNA-10a binds the 5′UTR of ribosomal protein mRNAs and enhances their translation. *Mol Cell* 30:460–471.
25. Parker R, Sheth U (2007) P bodies and the control of mRNA translation and degradation. *Mol Cell* 25:635–646.
26. Hornung V, et al. (2006) 5′-Triphosphate RNA is the ligand for RIG-I. *Science* 314: 994–997.
27. Zhou Z, et al. (2011) Antiviral activities of ISG20 in positive-strand RNA virus infections. *Virology* 409:175–188.
28. Sumpter R, Jr., et al. (2005) Regulating intracellular antiviral defense and permissiveness to hepatitis C virus RNA replication through a cellular RNA helicase, RIG-I. *J Virol* 79:2689–2699.
29. Vasudevan S, Tong Y, Steitz JA (2007) Switching from repression to activation: MicroRNAs can up-regulate translation. *Science* 318:1931–1934.
30. Vasudevan S, Tong Y, Steitz JA (2008) Cell-cycle control of microRNA-mediated translation regulation. *Cell Cycle* 7:1545–1549.
31. Shimakami T, et al. (2011) Protease inhibitor-resistant hepatitis C virus mutants with reduced fitness from impaired production of infectious virus. *Gastroenterology* 140: 667–675.

Therapeutics, Targets, and Chemical Biology

Cancer Research

Acyclic Retinoid Targets Platelet-Derived Growth Factor Signaling in the Prevention of Hepatic Fibrosis and Hepatocellular Carcinoma Development

Hikari Okada[1], Masao Honda[1,2], Jean S. Campbell[4], Yoshio Sakai[1], Taro Yamashita[1], Yuuki Takebuchi[1], Kazuhiro Hada[1], Takayoshi Shirasaki[1], Riuta Takabatake[1], Mikiko Nakamura[1], Hajime Sunagozaka[1], Takuji Tanaka[3], Nelson Fausto[4], and Shuichi Kaneko[1]

Abstract

Hepatocellular carcinoma (HCC) often develops in association with liver cirrhosis, and its high recurrence rate leads to poor patient prognosis. Although recent evidence suggests that peretinoin, a member of the acyclic retinoid family, may be an effective chemopreventive drug for HCC, published data about its effects on hepatic mesenchymal cells, such as stellate cells and endothelial cells, remain limited. Using a mouse model in which platelet-derived growth factor (PDGF)-C is overexpressed (*Pdgf-c Tg*), resulting in hepatic fibrosis, steatosis, and eventually, HCC development, we show that peretinoin significantly represses the development of hepatic fibrosis and tumors. Peretinoin inhibited the signaling pathways of fibrogenesis, angiogenesis, and Wnt/β-catenin in *Pdgf-c* transgenic mice. *In vitro*, peretinoin repressed the expression of PDGF receptors α/β in primary mouse hepatic stellate cells (HSC), hepatoma cells, fibroblasts, and endothelial cells. Peretinoin also inhibited PDGF-C–activated transformation of HSCs into myofibroblasts. Together, our findings show that PDGF signaling is a target of peretinoin in preventing the development of hepatic fibrosis and HCC. *Cancer Res; 72(17); 4459–71. ©2012 AACR.*

Introduction

Hepatocellular carcinoma (HCC) is one of the most common malignancies worldwide with a particularly poor patient outcome (1). It often develops as a result of chronic liver disease associated with hepatitis B or hepatitis C virus infection or with other etiologies such as long-term alcohol abuse, autoimmunity, and hemochromatosis (2–5). Despite the recent advances in antiviral therapy for hepatitis B or hepatitis C virus, these are insufficient to completely prevent the occurrence of HCC. Moreover, the recent increase in nonalcoholic fatty liver disease (NAFLD) associated with metabolic syndrome is a potential high-risk factor for the development of HCC (6).

HCC often develops during the advanced stages of liver fibrosis and is associated with deposits of extracellular matrix synthesized by activated stellate cells. During the course of chronic hepatitis, nonparenchymal cells, including Kupffer, endothelial, and activated stellate cells, release a variety of cytokines and growth factors. One of these growth factors is platelet-derived growth factor (PDGF), which is involved in fibrogenesis, angiogenesis, and tumorigenesis (7, 8). PDGF expression has been shown to be upregulated from the early stages of chronic hepatitis, suggesting its association with the development of fibrosis in chronic hepatitis C (CH-C; refs. 9 and 10). Overexpression of PDGF-C in mouse liver resulted in the progression of hepatic fibrosis, steatosis, and the development of HCC; this mouse model closely resembles the human HCC, which is frequently associated with hepatic fibrosis (7).

Peretinoin (generic name; code, NIK-333), developed by the Kowa Company, is an oral acyclic retinoid with a vitamin A–like structure, which targets the retinoid nuclear receptor. Oral administration of peretinoin was shown to significantly reduce the incidence of posttherapeutic HCC recurrence and improve the survival rates of patients in a clinical trial (11, 12). A large-scale clinical study including various countries is now planned to confirm its clinical efficacy.

Although peretinoin treatment can suppress HCC-derived cell line growth and inhibit experimental mouse or rat liver carcinogenesis (13, 14), the detailed mechanism of its effect has not been fully elucidated. Peretinoin has a high binding affinity to cellular retinoic acid-binding protein (15) and may interact with retinoic acid receptor-β and retinoid X receptor-α (16); however, the precise molecular targets for preventing HCC recurrence have not yet been elucidated.

Authors' Affiliations: [1]Department of Gastroenterology, Kanazawa University Graduate School of Medicine; [2]Department of Advanced Medical Technology, Kanazawa University Graduate School of Health Medicine; [3]Department of Oncologic Pathology, Kanazawa Medical University, Kanazawa, Japan; and [4]Department of Pathology, University of Washington School of Medicine, Seattle, Washington

Note: Supplementary data for this article are available at Cancer Research Online (http://cancerres.aacrjournals.org/).

Corresponding Author: Masao Honda, Department of Gastroenterology, Graduate School of Medicine, Kanazawa University, Takara-Machi 13-1, Kanazawa 920-8641, Japan. Phone: 81-76-265-2235; Fax: 81-76-234-4250; E-mail: mhonda@m-kanazawa.jp

doi: 10.1158/0008-5472.CAN-12-0028

In this study, we used PDGF-C transgenic (*Pdgf-c* Tg) mice to show that PDGF-C signaling is a possible target of peretinoin in the prevention of hepatic fibrosis, angiogenesis, and the development of HCC.

Materials and Methods

Chemicals

The acyclic retinoid peretinoin (generic name; code, NIK-333) [(2E,4E,6E,10E)-3,7,11,15-tetramethyl-2,4,6,10,14-hexadecapentaenoic acid, C20H30O2, molecular weight 302.46 g/mol] was supplied by Kowa Company.

Animal studies

The generation and characterization of *Pdgf-c Tg* have been described previously (7). Wild-type and *Pdgf-c Tg* mice on a C57BL/6J background were maintained in a pathogen-free animal facility under a standard 12-hour/12-hour light/dark cycle. After weaning at week 4, male mice were randomly divided into the following 3 groups: (1) *Pdgf-c Tg* or wild-type (WT) mice given a basal diet (CRF-1, Charles River Laboratories Japan), (2) *Pdgf-c Tg* or WT mice given a 0.03% peretinoin-containing diet, (3) *Pdgf-c Tg* or WT mice given a 0.06% peretinoin-containing diet. Control mice were normal male homozygotes. At week 20, mice were sacrificed to analyze the progression of hepatic fibrosis ($n = 15$ for each of the 3 groups). At week 48, mice were sacrificed to analyze the development of hepatic tumors ($n = 31$ for the basal diet group, $n = 37$ for the 0.03% peretinoin group, and $n = 17$ for the 0.06% peretinoin group). The incidence of hepatic tumors, maximum tumor size, and liver weight were evaluated. None of the treated WT mice given a diet of 0.03% peretinoin died, but death occurred in 5% of WT mice around after 36 weeks of age receiving a 0.06% peretinoin diet, probably because of its toxicity. In *Pdgf-c Tg* mice, death was observed at similar frequency as WT mice that received 0.06% peretinoin diet.

All animal experiments were carried out in accordance with Guidelines for the Care and Use of Laboratory Animals at the Takara-Machi Campus of Kanazawa University, Japan.

Cell culture

Human HCC cell lines Huh-7, HepG2, and HLE, the mouse fibroblast cell line NIH3T3, human umbilical vein endothelial cells (HUVEC), and human stellate cells Lx-2 (kindly provided by Dr. Scott Friedman, Mount Sinai School of Medicine, New York, NY) were maintained in Dulbecco's Modified Eagle Medium (DMEM; Gibco) supplemented with 10% FBS (Gibco), 1% L-glutamine (Gibco), and 1% penicillin/streptomycin (Gibco) in a humidified atmosphere of 5% CO_2 at 37°C. 1 to 5×10^4 cells were seeded in each well of a 12-well plate the day before serum starvation in serum-free DMEM for 8 hours. The culture medium was then replaced with serum-free medium containing peretinoin. After 24-hour incubation, cells were harvested for analysis.

Isolation and culture of mouse hepatic stellate cells

Hepatic stellate cells (HSC) were isolated from C57BL/6J mice and the effect of recombinant human PDGF-C and peretinoin on HSCs was evaluated *in vitro*. Pronase-collagenase liver digestion was used to isolate HSC from wild-type mice. All experiments were replicated at least twice. Freshly isolated HSCs suspended in culture medium were seeded in uncoated 24-well plates and incubated at 37°C in a humidified atmosphere of 5% CO_2 for 72 hours. Nonadherent cells were removed with a pipette and the culture medium was replaced with medium containing 80 ng/mL recombinant human PDGF-C (Abnova) with or without peretinoin or 9-*cis*-retinoic acid (9cRA; 5 or 10 μmol/L). Cells were harvested for analysis after 24-hour incubation.

Isolation of peripheral blood mononuclear cells

Peripheral blood mononuclear cells were harvested and labeled with FITC-conjugate CD34 (Cell Lab) and R-Phycoerythrin (PE)-conjugated CD31 antibodies (Cell Lab) for 30 minutes at 4°C. After washing with 1 mL PBS, CD31 and CD34 surface expression was measured with a FACSCalibur flow cytometer (BD Biosciences). All flow cytometric data were analyzed using FlowJo software (Tree Star).

Gene expression profiling

Gene expression profiling in mouse liver was evaluated using the GeneChip Mouse Genome 430 2.0 Array (Affymetrix). Liver tissue from WT, *Pdgf-c Tg*, and *Pdgf-c Tg* with 0.06% peretinoin mice all at weeks 20 and 48 was obtained and a total of 34 chip assays were conducted as described previously (17). Expression data have been deposited in the Gene Expression Omnibus (GEO; NCBI Accession; GSE31431).

Pathway analysis was conducted using MetaCore (GeneGo). Functional ontology enrichment analysis was conducted to compare the Gene Ontology (GO) process distribution of differentially expressed genes ($P < 0.01$; refs. 10 and 17). Direct interactions among differentially expressed genes between *Pdgf-c Tg* mice with or without peretinoin administration were examined as reported previously (10). Each connection represents a direct, experimentally confirmed, physical interaction (MetaCore).

Histopathology and immunohistochemical staining

Mouse liver tissues were fixed in 10% formalin and stained with hematoxylin and eosin. The liver neoplasms (HCC and liver cell adenoma) were diagnosed according to previously described criteria (18, 19). Hepatic fibrosis was evaluated by Azan staining. Percentages of fibrous areas were calculated microscopically using an image analysis system (BIOREVO BZ-9000: KEYENCE Japan). Immunohistochemical (IHC) staining was conducted by an immunoperoxidase technique with an Envision kit (DAKO). Primary antibodies used were: rabbit polyclonal PDGFR-α (1:100 dilution), PDGFR-β (1:100 dilution), VEGFR1 (1:100 dilution), desmin (1:100 dilution), β-catenin (1:200 dilution), and mouse monoclonal cyclin D1 (1:400 dilution; all from Cell Signaling Technology); collagen 1 (1:100 dilution), collagen 4 (1:100 dilution), CD31 (1:100 dilution), and CD34 (1:100 dilution; all from Abcam, Cambridge, MA); and Tie-2 (1:80 dilution) and Myc (1:100 dilution; both from Santa Cruz Biotechnology).

Quantitative real-time detection PCR

Total RNA was isolated from frozen liver tissue samples using a GenElute Mammalian Total RNA Miniprep Kit (Sigma-Aldrich) according to the manufacturer's protocol. cDNA was synthesized from 100 ng total RNA using a high-capacity cDNA reverse transcription kit (Applied Biosystems) then mixed with the TaqMan Universal Master Mix (Applied Biosystems) and each TaqMan probe. TaqMan probes used were PDGFR-α/β, VEGFR1/2, α-SMA, collagen 1/4, β-catenin, CyclinD1, and Myc (Applied Biosystems). Relative expression levels were calculated after normalization to glyceraldehyde-3-phosphate dehydrogenase (GAPDH).

Western blotting

Western blotting was conducted as described previously (20). Whole-cell lysates from mouse liver were prepared and lysed by CelLytic MT cell lysis reagent (Sigma-Aldrich) containing Complete Mini EDTA-free Protease Inhibitor cocktail tablets (Roche). Cytoplasmic and nuclear protein extracts were prepared using the NE-PER nuclear extraction reagent kit (Pierce Biotechnology). Primary antibodies used were PDGFR-α (1:1,000 dilution), PDGFR-β (1:1,000 dilution), VEGFR2 (1:1,000 dilution), p44/42 MAPK (1:1,000 dilution), total AKT (1:1,000 dilution), p-p44/42 MAPK (1:1,000 dilution), p-AKT (Ser473; 1:1,000 dilution), p-AKT (Thr308; 1:1,000 dilution), β-catenin (1:2,000 dilution), cyclin D1 (1:400 dilution), and lamin A/C (1:1,000 dilution; all Cell Signaling Technology); α-SMA (1:200 dilution; DAKO); 4-HNE (1:200 dilution; NOF); and GAPDH (1:1,000 dilution) and Myc (1:1,000 dilution; both Santa Cruz).

Statistical analysis

Results are expressed as mean ± SD. Significance was tested by 1-way analysis of variance with Bonferroni's method, and differences were considered statistically significant at $P < 0.05$.

Results

Peretinoin prevented the development of hepatic fibrosis in *Pdgf-c Tg*

To evaluate the HCC chemopreventive effects of peretinoin, we used a mouse model of *Pdgf-c Tg* in which PDGF-C is expressed under the control of the albumin promoter (7). Experimental mice were male mice expressing the PDGF-C transgene (*Pdgf-c Tg*); whereas male mice not expressing the transgene were considered WT. After weaning at week 4, *Pdgf-c Tg* or nontransgenic WT mice were fed a basal diet or a diet containing 0.03% or 0.06% peretinoin. At week 20, mice were sacrificed to analyze the progression of hepatic fibrosis. At week 48, mice were sacrificed to analyze the development of hepatic tumors (Fig. 1A). At week 20, Azan staining showed that predominant pericellular fibrosis had developed in *Pdgf-c Tg* mice (Fig. 1B). Densitometric analysis showed a significant dose-dependent reduction in the size of the fibrotic area in mice that received a diet containing peretinoin at both weeks 20 and 48 (Fig. 1C). Peretinoin therefore efficiently repressed the development of hepatic fibrosis in *Pdgf-c Tg* mice.

The expression of fibrosis-related genes in *Pdgf-c Tg* mice was evaluated by IHC staining, quantitative real-time detection PCR (RTD-PCR), and Western blotting. The expression of PDGFR-α and PDGFR-β, essential receptors for intracellular PDGF-C signaling, was upregulated mainly in the intracellular or portal area in *Pdgf-c Tg* mice livers (Fig. 2), but was significantly repressed by peretinoin after weaning at week 4. Similarly, the expression of collagen 1, collagen 4, and desmin was significantly upregulated in *Pdgf-c Tg* mice, but repressed by peretinoin (Fig. 2 and Supplementary Fig. S1A).

RTD-PCR results confirmed that these genes were substantially upregulated in *Pdgf-c Tg* mice and significantly repressed by both 0.03% and 0.06% peretinoin (Fig. 3A). Western blotting showed that the expression of phosphorylated extracellular signal-regulated kinase (p-ERK) 1/2 and cyclin D1, representative markers of the cell proliferation signaling pathway, was upregulated in *Pdgf-c Tg* mice, and repressed by peretinoin (Fig. 3B). Thus, peretinoin could partially but significantly prevent the development of hepatic fibrosis in *Pdgf-c Tg* mice during the study observation period of 48 weeks.

Peretinoin prevented the development of HCC in *Pdgf-c Tg* mice

At week 48, *Pdgf-c Tg* mice developed hepatic tumors with an incidence of 90% (Fig. 4A). Histologic assessment of these tumors verified that 54% (15/28) were adenomas and 46% (13/28) were HCC (Fig. 4A and C and Supplementary Fig. S2; ref. 21). Peretinoin (0.03%) dose-dependently repressed the incidence of hepatic tumors to 53% (19/36) and to 29% (5/17) at 0.06%. Correlating with tumor incidence, maximum tumor size and liver weight were also significantly repressed by peretinoin (Fig. 4B). Thus, peretinoin repressed the development of hepatic tumors in *Pdgf-c Tg* mice.

Serial gene expression profiling in the liver of *Pdgf-c Tg* mice that developed hepatic fibrosis and tumors

To examine which signaling pathways were altered during the progression of hepatic fibrosis and tumor development, we analyzed gene expression profiling in the liver of *Pdgf-c Tg* mice using Affymetrix gene chips. By filtering criteria for $P < 0.001$ and more than 2-fold differences, 538 genes were selected as differentially expressed. One-way hierarchical clustering analysis of differentially expressed genes is shown in Supplementary Fig. S3.

Of the 3 main clusters, 2 were upregulated (clusters A and B) and 1 was downregulated (cluster C). Cluster A consisted of immune-related [chemokine (C-C motif) receptor (CCR)4, CCR2, toll-like receptor (TLR)3 and TLR4], apoptosis-related [caspase (CASP)1 and CASP9], angiogenesis- and/or growth factor–related (PDGF-C, VEGF-C, osteopontin, HGF), oncogene-related [v-ets erythroblastosis virus E26 oncogene homologue (Ets)1, Ets2, CD44, N-myc downstream-regulated (NDRG)1], and fibrosis-related (tubulin) genes. The expression of cluster A genes was further upregulated in tumors at week

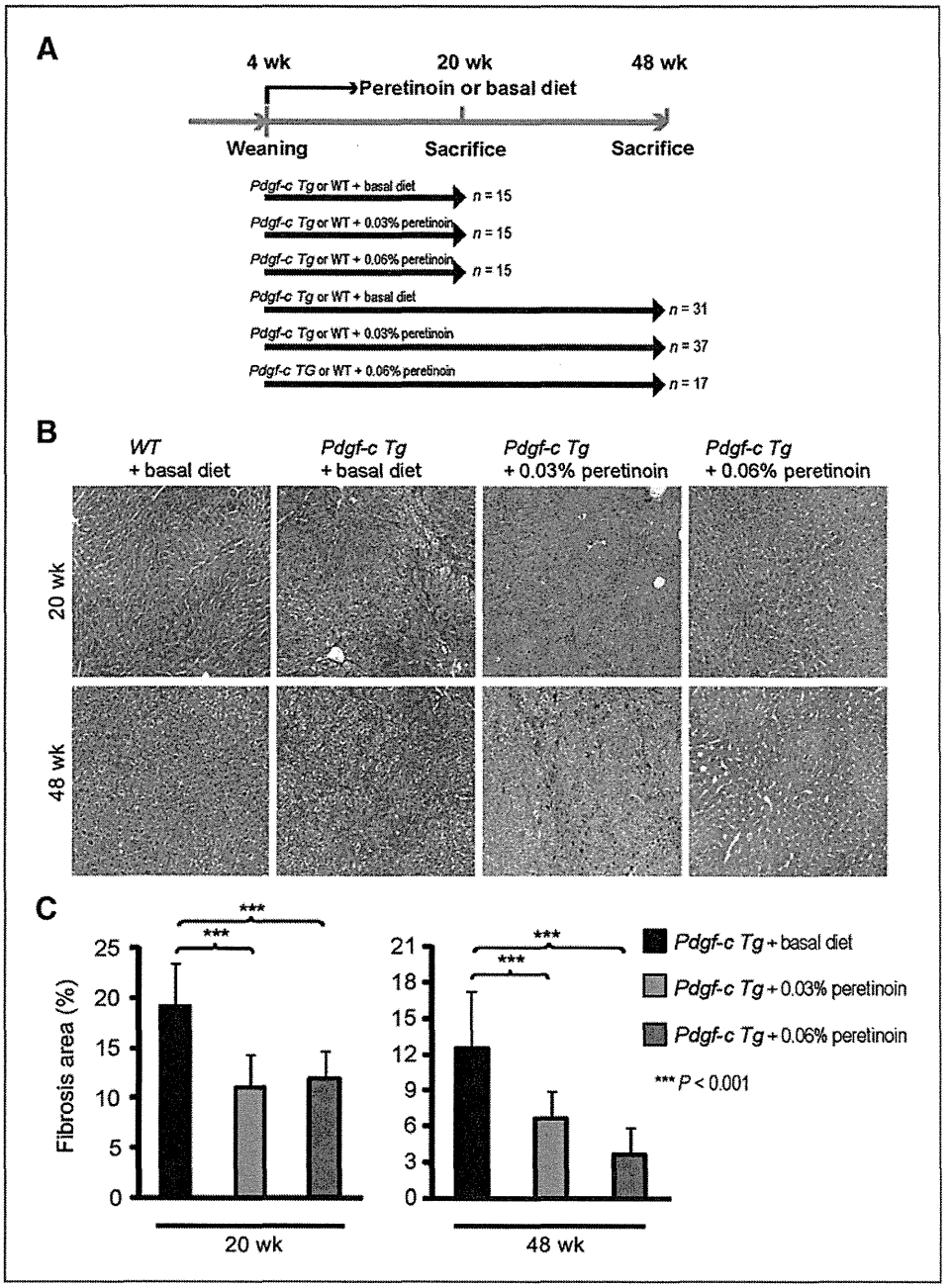

Figure 1. A, feeding schedule of *Pdgf-c Tg* and WT mice. After weaning, male mice were randomly divided into 3 groups: (i) *Pdgf-c Tg* or WT mice receiving basal diet, (ii) *Pdgf-c Tg* or WT mice receiving 0.03% peretinoin-containing diet, and (iii) *Pdgf-c Tg* or WT mice receiving 0.06% peretinoin-containing diet. B, Azan staining of WT or *Pdgf-c Tg* mouse livers fed with different diets at 20 weeks and 48 weeks. C, densitometric analysis of *Pdgf-c Tg* mouse liver fibrotic areas at 20 weeks ($n = 15$) and 48 weeks ($n = 15$).

48. Cluster B consisted mainly of connective tissue- and/or fibrosis-related [vascular cell adhesion molecule (VCAM)1, collagen I, III, IV, V, VI, integrin, decorin, TGF-βRII, PDGFR-α, and PDGFR-β] genes, the expression of which declined slightly at week 48. In contrast, cluster C, containing differentiation and liver function related genes [cytochrome P450, family 2, subfamily c (CYP2C)], were downregulated during the course of hepatic fibrosis and tumor development (Supplementary Fig. S4). Cluster C included xenobiotic- and metabolic process–related genes, which are potential targets of peretinoin. Peretinoin treatment prevented hepatic fibrosis and it preserved liver function. In addition, peretinoin might induce its target genes. Thus, peretinoin reduced the expression of upregulated genes (clusters A and B) and restored the expression of downregulated genes (cluster C) at both weeks 20 and 48 (Supplementary Figs. S3 and S4).

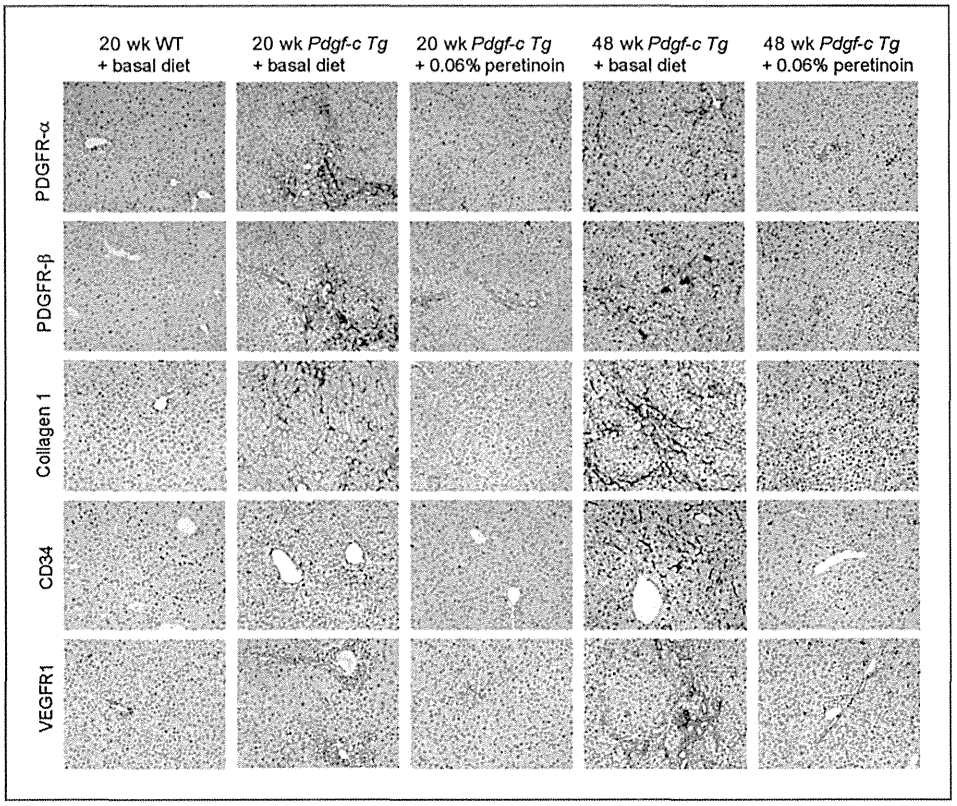

Figure 2. IHC staining of PDGFR-α, PDGFR-β, collagen 1, CD34, and VEGFR1 expression in *Pdgf-c Tg* or WT mouse livers fed a basal diet or 0.06% peretinoin.

To examine the molecular network consisting of differentially expressed genes in *Pdgf-c Tg* mice with or without peretinoin administration, the direct interactions of 513 genes were analyzed by MetaCore (i.e., 413 genes were downregulated and 100 genes were upregulated in *Pdgf-c Tg* mice treated with peretinoin compared with untreated mice; $P < 0.002$). A core gene network consisting of 41 genes was obtained (Supplementary Fig. S5) including interactions between representative growth factors, receptors (PDGFR and TGFβR), and transcriptional factors. Of these genes, the transcriptional factors Sp1 and Ap1 seem to be key regulators in the network (Supplementary Fig. S5).

Peretinoin inhibits PDGFR *in vitro*

Gene expression profiling landscaped the dynamic changes of signaling pathways in *Pdgf-c Tg* mice. To determine the effects of peretinoin *in vitro*, primary HSCs from normal C57BL/6J mice were stimulated by PDGF-C (Fig. 5) to induce the expression of PDGFR-α, PDGFR-β, alpha smooth muscle actin (α-SMA), and collagen 1a2; activated HSCs thus transformed into myofibroblasts (Fig. 5A and B). Peretinoin significantly reduced the expression of these genes and inhibited HSC activation.

We next evaluated the effects of peretinoin on human hepatoma cell lines (Huh-7, HepG2, and HLE), mouse embryonic fibroblast cells (NIH3T3), HUVECs, and Lx-2 (ref. 22; Supplementary Fig. S6A). Experimental conditions were optimized so that more than 90% of cells were variable at 20 μmol/L peretinoin, as determined by an MTS cell proliferation assay (data not shown). Peretinoin dose-dependently inhibited the expression of PDGFR-α and PDGFR-β in Huh-7, HepG2, HLE, NIH3T3, HUVEC, and Lx-2 cells, whereas no obvious expression of PDGFR-α was observed in HepG2 cells and HUVECs (Supplementary Fig. S6A). Peretinoin also inhibited VEGFR2 expression in HUVEC. These results were confirmed by RTD-PCR (data not shown). Correlating with these results, the expression of phosphorylated serine/threonine kinase AKT (p-AKT) and p-ERK1/2, downstream signaling molecules of PDGFR-α, PDGFR-β, and VEGFR2, was also dose-dependently repressed. The expression of collagen 1a2 was significantly repressed by peretinoin in Lx-2, HLE, and Huh-7 cells (Supplementary Fig. S6B). These results suggest that peretinoin may inhibit hepatic fibrosis, angiogenesis, and tumor growth through reduction of the PDGF and VEGF signaling pathway.

We examined the expression of 2 key regulators in peretinoin signaling, Sp1 and Ap1, in Huh-7 cells. Interestingly, the expression of Sp1 was decreased, which correlates with that of PDGFR-α, whereas expression of phosphorylated c-Jun (p-c-Jun) was increased in Huh-7 cells (Supplementary Fig. S6C). Therefore, peretinoin seems to repress the expression of PDGFR, partially through the inhibition of Sp1.

Peretinoin inhibits hepatic angiogenesis in *Pdgf-c Tg* mice

The effect of peretinoin on liver angiogenesis in *Pdgf-c Tg* mice was further analyzed. IHC staining of *Pdgf-c Tg* mouse

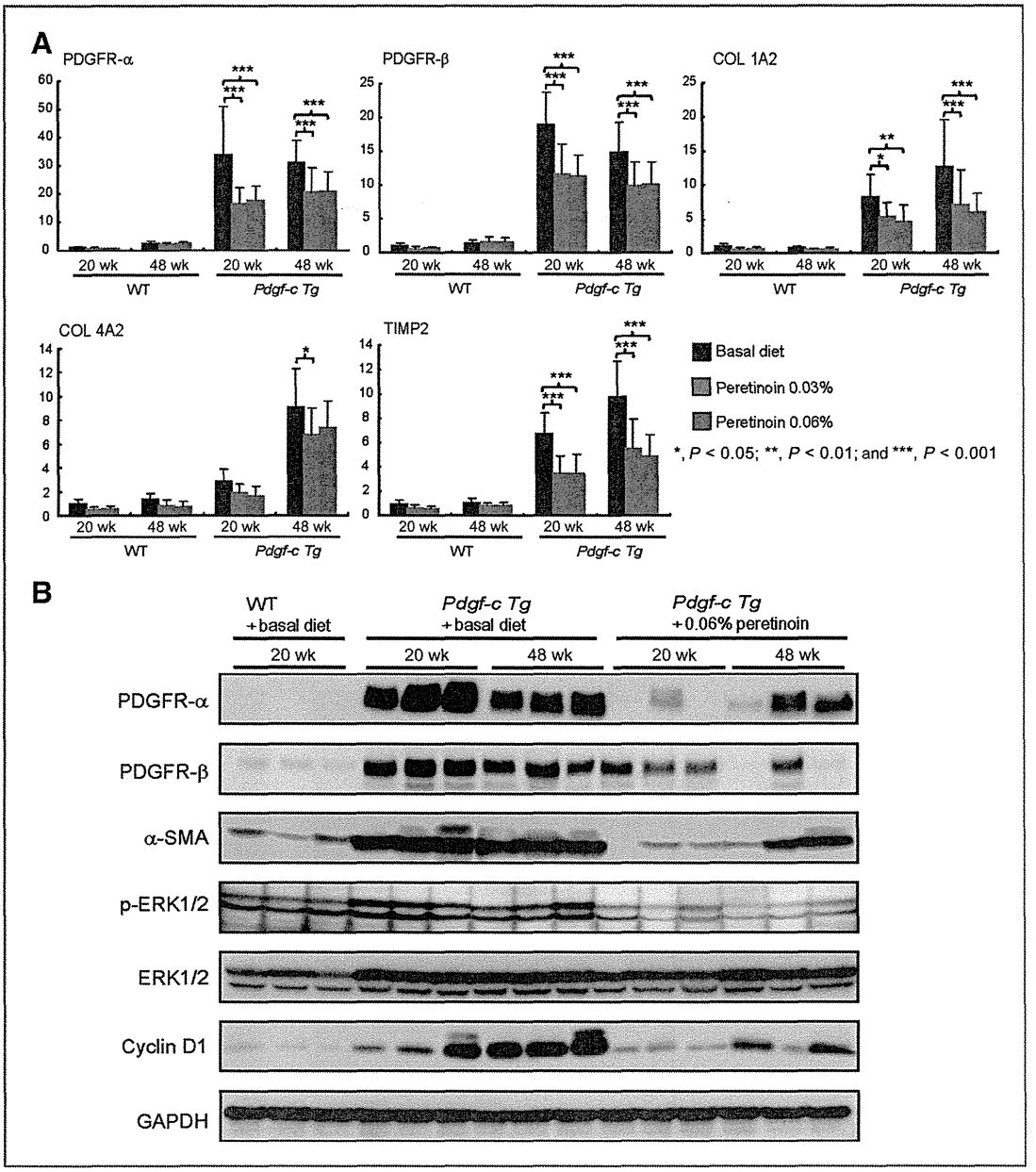

Figure 3. A, RTD-PCR analysis of PDGFR-α, PDGFR-β, collagen (COL) 1a2, collagen 4 a2, and TIMP2 expression in *Pdgf-c Tg* ($n = 5$) or WT mouse livers ($n = 15$). B, Western blotting of PDGFR-α, PDGFR-β, α-SMA, p-ERK, ERK, cyclin D1, and GAPDH expression in PDGF-C Tg or WT mouse livers fed a basal diet or 0.06% peretinoin at 20 or 48 weeks ($n = 3$).

livers at weeks 20 and 48 revealed overexpression of the endothelial markers CD31 and CD34 and the endothelial growth factors VEGFR1 and endothelium-specific receptor tyrosine kinase 2 (Tie2) in the mesenchymal region (Fig. 6 and Supplementary Fig. S1A). This expression was significantly repressed by peretinoin as determined by the densitometric area (Supplemental Fig. S1B). RTD-PCR results revealed significant upregulation of VEGFR1 (Flt-1) in *Pdgf-c Tg* mice compared with WT mice at both weeks 20 and 48, whereas the expression of VEGFR2 (Flk-1) and Tie2 was only upregulated at week 48. The expression of these genes was significantly repressed by peretinoin (Fig. 6A). Western blotting confirmed the upregulation of CD31 and VEGFR1 (Flk-1) at week 48 (Fig. 6B). In addition, p-AKT (Thr 308 and Ser 473) and 4-hydroxy-2-nonenal (4-HNE), an oxidative stress marker, were upregulated in *Pdgf-c Tg* mice and repressed by peretinoin (Fig. 6B).

We also assessed circulating endothelial cells (CEC), a useful biomarker for angiogenesis in the blood, and found that the $CD31^+/CD34^+$ CEC population was significantly upregulated in *Pdgf-c Tg* mice at week 48 but significantly repressed by peretinoin (Fig. 6C and D). Thus, peretinoin

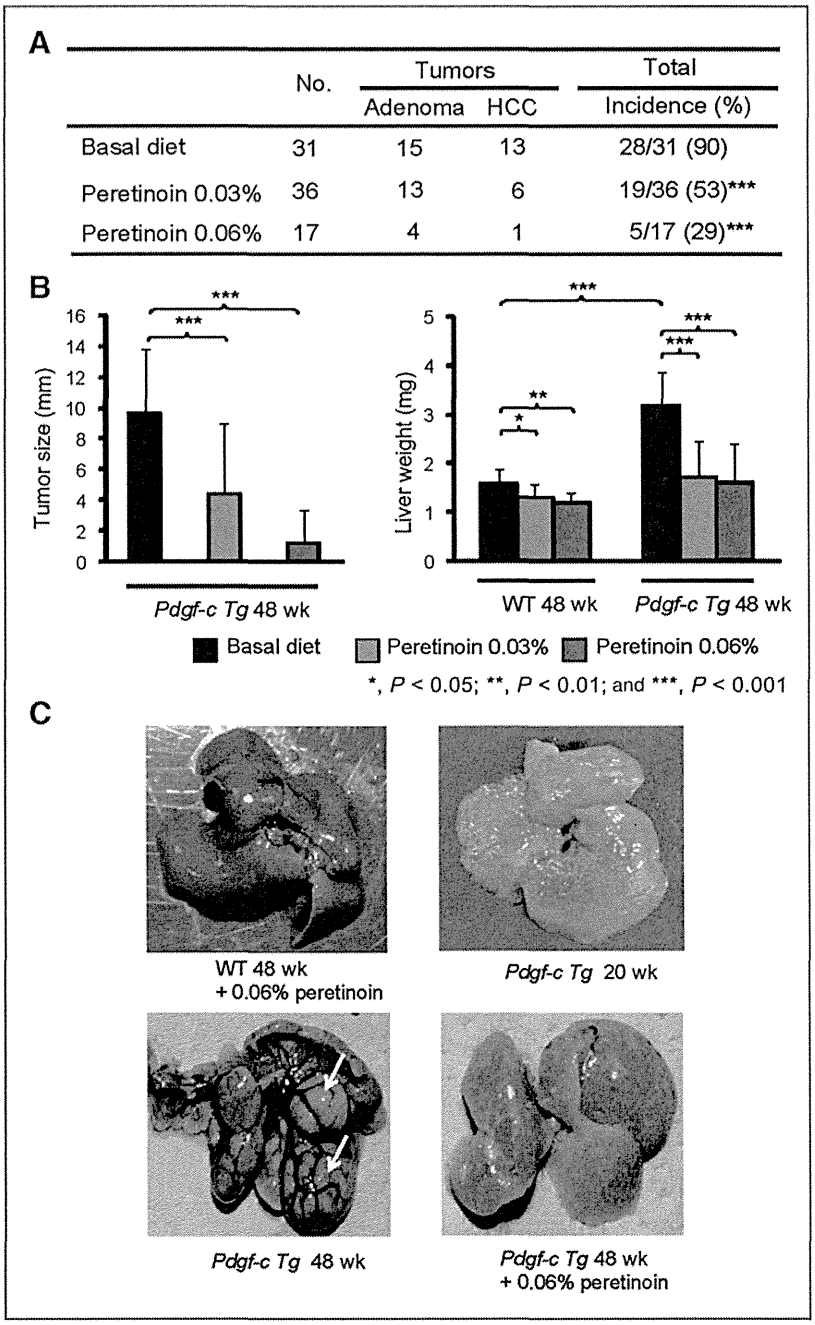

Figure 4. A, incidence of hepatic tumors (adenoma or HCC) in *Pdgf-c Tg* mouse livers fed with different diets. B, tumor sizes and liver weights of *Pdgf-c Tg* and WT mice fed with basal diet ($n = 31$ for *Pdgf-c* Tg, $n = 15$ for WT mice) or 0.03% ($n = 36$ for *Pdgf-c* Tg, $n = 15$ for WT mice) and 0.06% ($n = 17$ for *Pdgf-c* Tg, $n = 15$ for WT mice) peretinoin at 48 weeks. C, macroscopic findings of *Pdgf-c Tg* or WT mouse livers. No obvious change was observed in the liver of WT mice fed with 0.06% peretinoin for 48 weeks (top left). Fibrosis and steatosis were observed in the liver of *Pdgf-c Tg* mice fed a basal diet for 20 weeks (top right). Multiple tumors developed (white arrows) in the liver of *Pdgf-c Tg* mice fed a basal diet for 48 weeks (bottom left). Suppression of tumor development in the liver of *Pdgf-c Tg* mice fed a 0.06% peretinoin diet for 48 weeks (bottom right).

seems to inhibit angiogenesis in the liver of *Pdgf-c Tg* mice, which might prevent the development of hepatic tumors.

Peretinoin inhibits canonical Wnt/β-catenin signaling in *Pdgf-c Tg* mice

The activation of the Wnt/β-catenin signaling pathway is seen in 17% to 40% of patients with primary HCC (23, 24). Moreover, recent reports suggested an interaction between PDGF signaling and Wnt/β-catenin signaling (25–27). We evaluated Wnt/β-catenin signaling in *Pdgf-c Tg* mice and showed by IHC staining that β-catenin was overexpressed in the submembrane at week 48 (Fig. 7A). Peretinoin significantly reduced this expression (Fig. 7A and B), and Western blotting revealed that accumulation of β-catenin in the nuclear fraction of liver tumor tissues was more preferentially repressed by peretinoin than in the cytoplasmic fraction, although expression was repressed in both fractions (Fig. 7C). Wnt ligand (Wnt5a) and frizzled receptor (Fzd1) expression was significantly upregulated in hepatic tumors compared with normal liver (Fig. 7D). These results together suggest that canonical Wnt/β-catenin

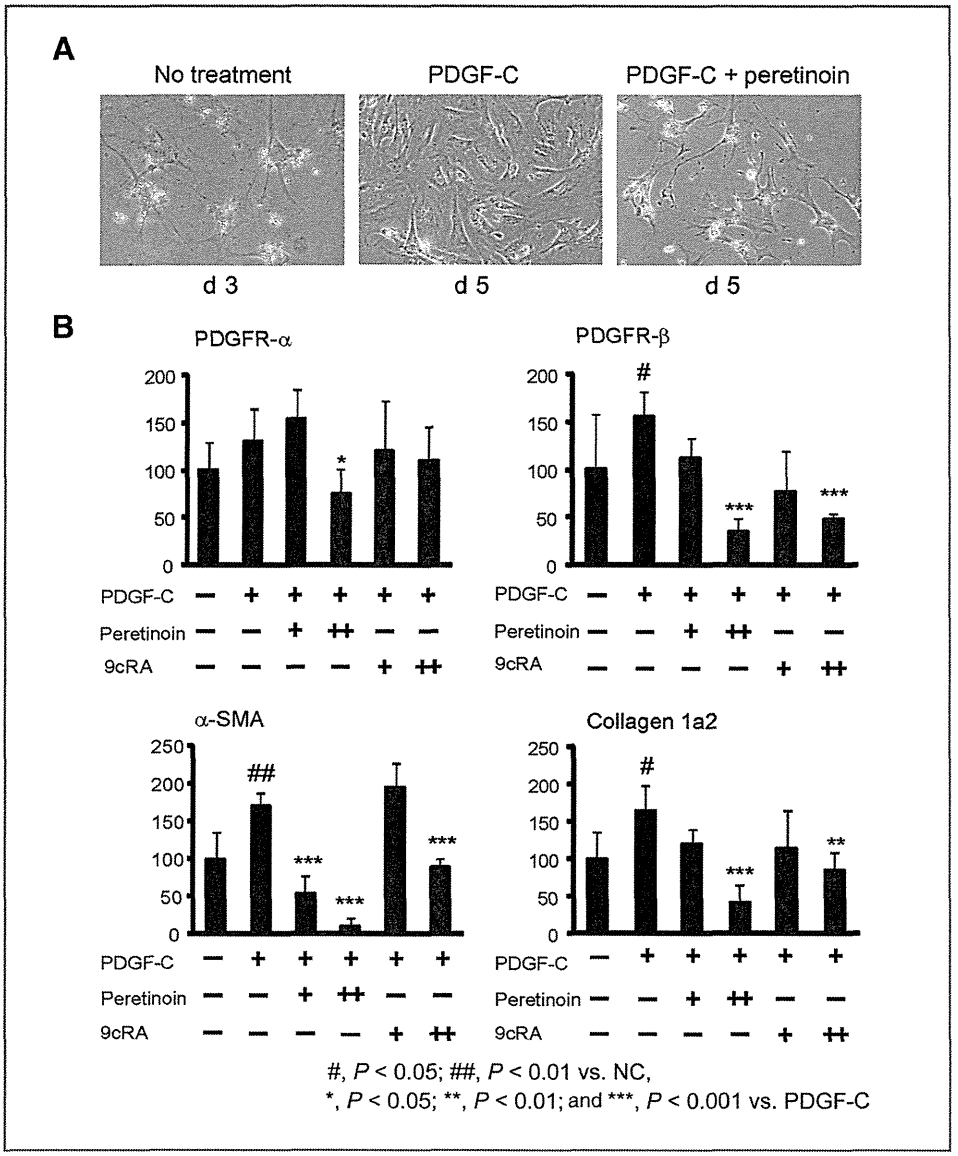

Figure 5. A, microscopic view of freshly isolated primary mouse HSCs after PDGF-C transformation into myofibroblasts (left). Peretinoin inhibited the transformation of HSCs by PDGF-C. B, RTD-PCR analysis of PDGFR-α, PDGFR-β, α-SMA, and collagen 1a2 expression in HSCs treated with or without PDGF-C, peretinoin, and 9cRA ($n = 4$). PDGF-C (+), 80 ng/mL; peretinoin (+), 5 μmol/L; (++), 10 μmol/L; 9cRA (+), 5 μmol/L; (++), 10 μmol/L. NC, no control.

signaling is activated in hepatic tumors and repressed by peretinoin.

Growth factors such as PDGF or HGF potentially activate Wnt/β-catenin signaling (26, 28), which promotes cancer progression and metastasis. We evaluated whether such growth factor signaling could be repressed by peretinoin in hepatic tumors. The expression of c-myc, β-catenin, Tie2, Fit-1, and Flk-1 were significantly upregulated from 1.5- to 4-fold in hepatic tumors compared with normal liver, and this expression was significantly repressed by peretinoin. Similarly, the expression of PDGFR-α, PDGFR-β, collagen 1a2, collagen 4a2, tissue inhibitor of metalloproteinase 2 (TIMP2), and cyclin D1 was substantially upregulated from 5- to 15-fold in hepatic tumors, and significantly repressed by peretinoin (Fig. 7D). Thus, growth factor signaling as well as canonical Wnt/β-catenin signaling in hepatic tumors seems to be repressed by peretinoin. These results explain the inhibitory effect of peretinoin in the development of HCC in *Pdgf-c Tg* mice.

Discussion

HCC often develops in association with liver cirrhosis and its high recurrence rate leads to poor patient prognosis. Indeed, the 10-year recurrence-free survival rate after liver resection for HCC with curative intent was shown to be only 20% (29). Therefore, there is a pressing need to develop effective preventive therapy for HCC recurrence to improve its prognosis.

Peretinoin, a member of the acyclic retinoid family, is expected to be an effective chemopreventive drug for HCC (11, 12, 30) as shown by a previous phase II/III trial in which 600 mg peretinoin per day in the Child-Pugh A subgroup reduced the risk of HCC recurrence or death by 40% [HR = 0.60 (95% CI, 0.40–0.89); ref. 31]. However, further clinical

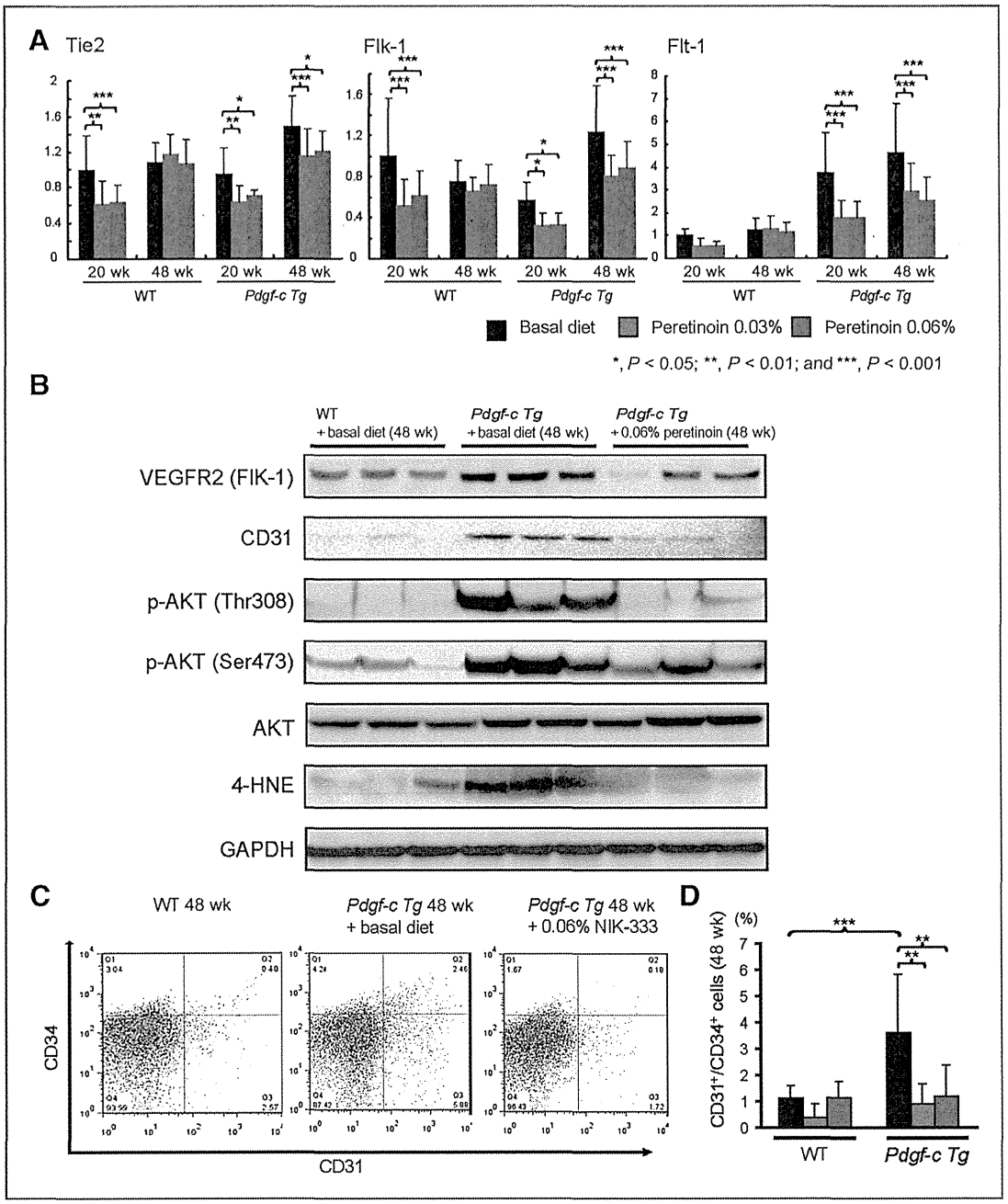

Figure 6. A, RTD-PCR analysis of Tie2, Flk-1, and Flt-1 expression in the liver of *Pdgf-c Tg* and WT mice fed with different diets ($n = 15$). B, Western blotting of Flk-1, CD31, p-AKT (Thr 308, Ser473), AKT, 4-HNE, and GAPDH expression in the liver of *Pdgf-c Tg* or WT mice fed a basal diet or 0.06% peretinoin at 48 weeks ($n = 3$). C, fluorescence-activated cell-sorting analysis of CD31- and CD34-positive CEC in blood of *Pdgf-c Tg* or WT mice fed a basal diet or 0.06% peretinoin at 48 weeks. D, frequency of CD31- and CD34-positive CEC in blood of *Pdgf-c Tg* or WT mice fed a basal diet or 0.06% peretinoin at 48 weeks ($n = 10$).

studies are needed to confirm the clinical efficacy of peretinoin, and a large scale study involving several countries is currently being planned.

During the course of chronic hepatitis, nonparenchymal cells including Kupffer, endothelial and activated stellate cells release a variety of cytokines and growth factors that might accelerate hepatocarcinogenesis. Although peretinoin has been shown to suppress the growth of HCC-derived cells by inducing apoptosis and differentiation (32–35), increasing p21 and reducing cyclin D1 (13), limited data have been published about its effects on hepatic mesenchymal cells such as stellate cells and endothelial cells (14).

In parallel with a phase II/III trial, we conducted a pharmacokinetics study of peretinoin focusing on 12

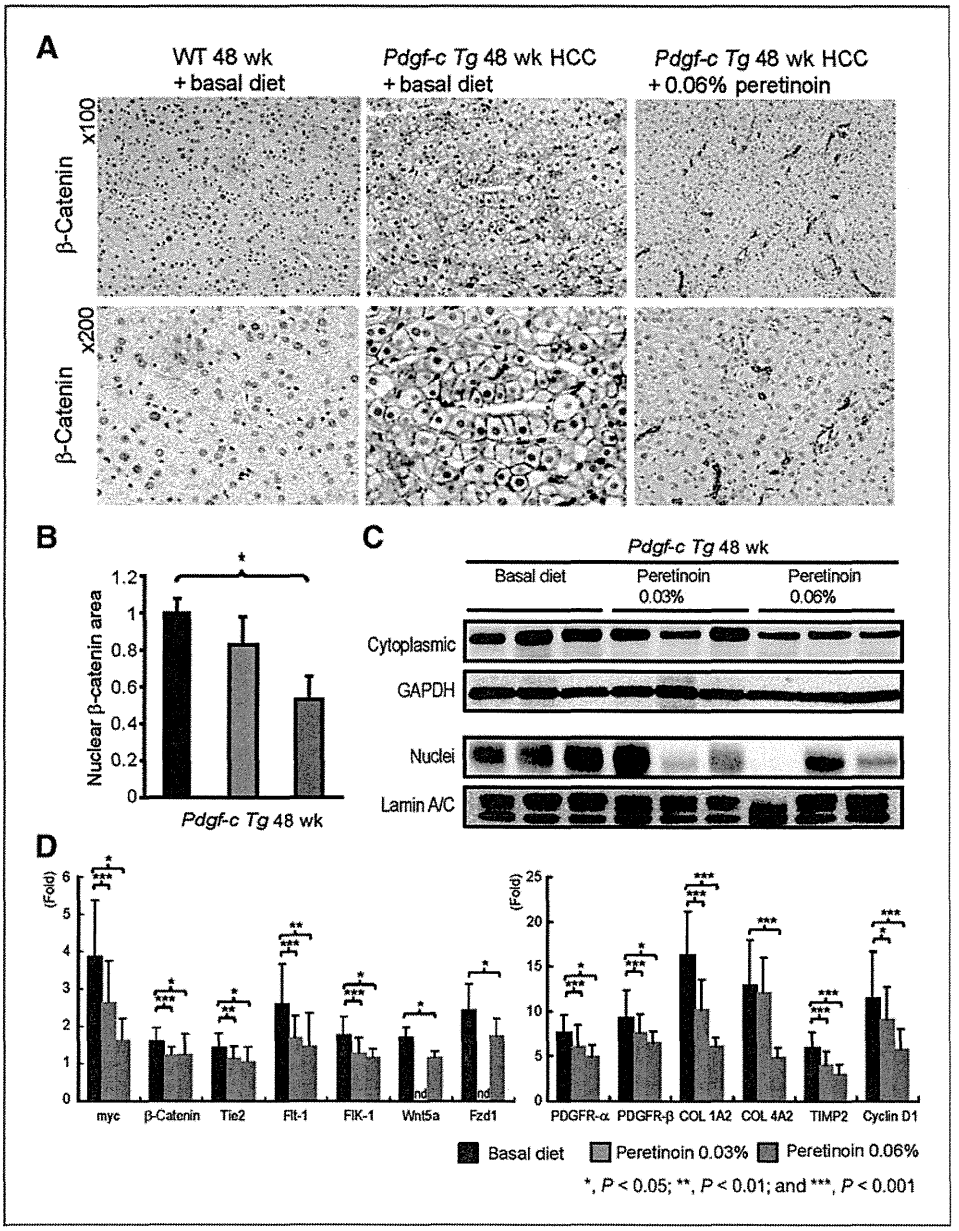

Figure 7. A, IHC staining of β-catenin expression in HCC tissues of *Pdgf-c Tg* mice fed a basal diet or 0.06% peretinoin at 48 weeks. B, densitometric analysis of β-catenin expression in the liver of *Pdgf-c Tg* mice fed with different diets ($n = 15$ for basal diet, $n = 15$ for 0.03% peretinoin, $n = 5$ for 0.06% peretinoin). C, Western blotting of β-catenin expression in cytoplasmic and nuclear fractions of *Pdgf-c Tg* mouse livers fed with different diets. GAPDH was used to standardize cytoplasmic protein and lamin A/C to standardize nuclear protein ($n = 3$). D, RTD-PCR analysis of myc, β-catenin, Tie2, Flt-1, Flk-1, Wnt5a, Fzd1, PDGFR-α, PDGFR-β, collagen (COL) 1a2, collagen 4a2, TIMP2, and cyclin D1 expression in HCC tissues of *Pdgf-c Tg* mice fed with different diets ($n = 15$ for basal diet, $n = 15$ for 0.03% peretinoin, $n = 5$ for 0.06% peretinoin). Relative fold expressions compared with WT mice are shown.

patients with CH-C and HCC to monitor the biological behavior of peretinoin in the liver. Gene expression profiling during peretinoin administration revealed that HCC recurrence within 2 years could be predicted and that PDGF-C expression was one of the strongest predictors. In addition, other genes related to angiogenesis, cancer stem cell and tumor progression were downregulated, whereas expression of genes related to hepatocyte differentiation and tumor suppression was upregulated by peretinoin (data not shown). Moreover, a recent report revealed the emerging significance of PDGF-C–mediated angiogenic and tumorigenic properties (7, 8, 36). In this study, we therefore used the mouse model of *Pdgf-c Tg*, which displays the phenotypes of hepatic fibrosis, steatosis, and HCC development that resemble human HCC arising from chronic hepatitis usually associated with advanced hepatic fibrosis.

We showed that peretinoin effectively inhibits the progression of hepatic fibrosis and tumors in *Pdgf-c Tg* mice (Figs. 1 and 4). Affymetrix gene chips analysis revealed dynamic changes in hepatic gene expression (Supplementary Fig. S3), which were confirmed by IHC staining, RTD-PCR and Western blotting. Pathway analysis of differentially expressed genes suggested that the transcriptional regulators Sp1 and Ap1 are key regulators in the peretinoin inhibition of hepatic fibrosis and tumor development in *Pdgf-c Tg* mice (Supplementary Fig. S5).

We clearly showed that peretinoin inhibited PDGF signaling through the inhibition of PDGFRs (Figs. 2 and 3). In

addition, we showed that PDGFR repression by peretinoin inhibited primary stellate cell activation (Fig. 5). Interestingly, this inhibitory effect was more pronounced than the effects of 9cRA (Fig. 5B). Normal mouse and human hepatocytes neither express PDGF receptors (J.S. Campbell and N. Fausto, unpublished data), nor proliferate in response to treatment with PDGF ligands (7). However, peretinoin inhibited the expression of PDGFRs, collagens, and their downstream signaling molecules in cell lines of hepatoma (Huh-7, HepG2, and HLE), fibroblast (NIH3T3), endothelial cells (HUVEC), and stellate cells (Lx-2; Supplementary Fig. S6). Furthermore, Sp1 but not Ap1, might be involved in the repression of PDGFR-α in Huh-7 cells (Supplementary Fig. 6C). The overexpression of Sp1-activated PDGFR-α promoter activity, whereas siRNA knockdown of Sp1 repressed PDGFR-α promoter activity in Huh-7 cells (data not shown). Therefore, this seems to confirm that Sp1 is involved in the regulation of PDGFR, as reported previously (37, 38), although these findings should be further investigated in different cell lines. A recent report showed the involvement of transglutaminase 2, caspase3, and Sp1 in peretinoin signaling (35).

Peretinoin was shown to inhibit angiogenesis in the liver of *Pdgf-c Tg* mice in this study, as shown by the decreased expression of VEGFR1/2 and Tie 2 (Figs. 2 and 6 and Supplementary Fig. S1). Moreover, peretinoin inhibited the number of $CD31^+$ and $CD34^+$ endothelial cells (CEC) in the blood and liver (Fig. 6C and D), while also inhibiting the expression of EGFR, c-kit, PDGFRs, and VEGFR1/2 in *Pdgf-c Tg* mice (data not shown). We also showed that peretinoin inhibited the expression of multiple growth factors such as HGF, IGF, VEGF, PDGF, and HDGF, which were upregulated from 3- to 10-fold in *Pdgf-c Tg* mice (Supplementary Fig. S3). These activities collectively might contribute to the antitumor effect of peretinoin in *Pdgf-c Tg* mice. The inhibition of both PDGFRs and VEGFR signaling by peretinoin was previously shown to have a significant effect on tumor growth (36), and we confirmed herein that peretinoin inhibited the expression of VEGFR2 in HUVECs (Supplementary Fig. S6; ref. 39). Finally, we showed that peretinoin inhibited canonical Wnt/β-catenin signaling by showing the decreased nuclear accumulation of β-catenin (Fig. 7). These data confirm the previous hypothesis of transrepression of the β-catenin promoter by 9cRA *in vitro* (40).

Although we showed that the PDGF signaling pathway is a target of peretinoin for preventing the development of hepatic fibrosis and tumors in mice, retinoid-inducing genes such as G0S2 (41), TGM2 (35), CEBPA (42), ATF, TP53BP, metallothionein 1H (MT1H), MT2A, and hemopexin (HPX) were upregulated in peretinoin-treated mice (data not shown). These canonical retinoid pathways are likely to participate in preventing disease progression in conjunction with anti-PDGF effects.

The precise mechanism of peretinoin toxicity, in which 5% of mice treated with 0.06% peretinoin died after 24 weeks of treatment, is currently under investigation. These mice showed severe osteopenia and we speculate that the toxicity might be caused by retinoid-induced osteopenia, as observed in a hypervitaminosis A rat model (43). However, the toxicity of prolonged treatment with oral retinoids in humans remains controversial (44) and severe osteopenia has so far only been seen in a rodent model.

In summary, we show that peretinoin effectively inhibits hepatic fibrosis and HCC development in *Pdgf-c Tg* mice. Further studies are needed to elucidate the detailed molecular mechanisms of peretinoin action and the effect of peretinoin on PDGF-C in human HCC. The recently developed multikinase inhibitor Sorafenib (BAY 43-9006, Nexavar) was shown to improve the prognosis of patients with advanced HCC (45). Promisingly, a phase II/III trial of peretinoin showed it to be safe and well tolerated (46). Therefore, combinatorial therapy that incorporates the use of small molecule inhibitors with peretinoin may be beneficial to some patients. The application of peretinoin during pre- or early-fibrosis stage could be beneficial in preventing the progression of fibrosis and subsequent development of HCC in patients with chronic liver disease.

Disclosure of Potential Conflicts of Interest

No potential conflicts of interest were disclosed.

Authors' Contributions

Conception and design: M. Honda, J.S. Campbell, S. Kaneko
Acquisition of data (provided animals, acquired and managed patients, provided facilities, etc.): H. Okada, M. Honda, J.S. Campbell, Y. Sakai, T. Yamashita, Y. Takebuchi, K. Hada, T. Shirasaki, R. Takabatake, M. Nakamura, H. Sunagozaka, N. Fausto
Analysis and interpretation of data (e.g., statistical analysis, biostatistics, computational analysis): J.S. Campbell, T. Yamashita, H. Sunagozaka, S Kaneko
Writing, review, and/or revision of the manuscript: H. OkadaM. Honda, J.S. Campbell, N. Fausto, S. Kaneko
Study supervision: J.S. Campbell, S. Kaneko
Pathologic examination and evaluation: T. Tanaka

Acknowledgments

The authors thank Dr. Scott Friedman, Mount Sinai School of Medicine (New York, NY), for providing Lx-2 cell lines and Nami Nishiyama and Masayo Baba for their excellent technical assistance.

Grant Support

This work was funded by NIH grants CA-23226, CA-174131, and CA-127228 (J.S. Campbell and N. Fausto). This work was also supported in part by a grant-in-aid from the Ministry of Health, Labour and Welfare, and KOWA Co., Ltd., Tokyo, Japan (M. Honda and colleagues).

The costs of publication of this article were defrayed in part by the payment of page charges. This article must therefore be hereby marked *advertisement* in accordance with 18 U.S.C. Section 1734 solely to indicate this fact.

Received January 9, 2012; revised April 27, 2012; accepted May 18, 2012; published OnlineFirst May 31, 2012.

References

1. Befeler AS, Di Bisceglie AM. Hepatocellular carcinoma: diagnosis and treatment. Gastroenterology 2002;122:1609–19.

2. Mohamed AE, Kew MC, Groeneveld HT. Alcohol consumption as a risk factor for hepatocellular carcinoma in urban southern African blacks. Int J Cancer 1992;51:537–41.

3. Tsukuma H, Hiyama T, Tanaka S, Nakao M, Yabuuchi T, Kitamura T, et al. Risk factors for hepatocellular carcinoma among patients with chronic liver disease. N Engl J Med 1993; 328:1797–801.
4. Deugnier YM, Charalambous P, Le Quilleuc D, Turlin B, Searle J, Brissot P, et al. Preneoplastic significance of hepatic iron-free foci in genetic hemochromatosis: a study of 185 patients. Hepatology 1993;18:1363–9.
5. Yeoman AD, Al-Chalabi T, Karani JB, Quaglia A, Devlin J, Mieli-Vergani G, et al. Evaluation of risk factors in the development of hepatocellular carcinoma in autoimmune hepatitis: implications for follow-up and screening. Hepatology 2008;48:863–70.
6. Smedile A, Bugianesi E. Steatosis and hepatocellular carcinoma risk. Eur Rev Med Pharmacol Sci 2005;9:291–3.
7. Campbell JS, Hughes SD, Gilbertson DG, Palmer TE, Holdren MS, Haran AC, et al. Platelet-derived growth factor C induces liver fibrosis, steatosis, and hepatocellular carcinoma. Proc Natl Acad Sci U S A 2005;102:3389–94.
8. Crawford Y, Kasman I, Yu L, Zhong C, Wu X, Modrusan Z, et al. PDGF-C mediates the angiogenic and tumorigenic properties of fibroblasts associated with tumors refractory to anti-VEGF treatment. Cancer Cell 2009;15:21–34.
9. Lau DT, Luxon BA, Xiao SY, Beard MR, Lemon SM. Intrahepatic gene expression profiles and alpha-smooth muscle actin patterns in hepatitis C virus induced fibrosis. Hepatology 2005;42: 273–81.
10. Honda M, Yamashita T, Ueda T, Takatori H, Nishino R, Kaneko S. Different signaling pathways in the livers of patients with chronic hepatitis B or chronic hepatitis C. Hepatology 2006;44: 1122–38.
11. Muto Y, Moriwaki H, Ninomiya M, Adachi S, Saito A, Takasaki KT, et al. Prevention of second primary tumors by an acyclic retinoid, polyprenoic acid, in patients with hepatocellular carcinoma. Hepatoma Prevention Study Group. N Engl J Med 1996;334:1561–7.
12. Muto Y, Moriwaki H, Saito A. Prevention of second primary tumors by an acyclic retinoid in patients with hepatocellular carcinoma. N Engl J Med 1999;340:1046–7.
13. Suzui M, Masuda M, Lim JT, Albanese C, Pestell RG, Weinstein IB. Growth inhibition of human hepatoma cells by acyclic retinoid is associated with induction of p21(CIP1) and inhibition of expression of cyclin D1. Cancer Res 2002;62:3997–4006.
14. Sano T, Kagawa M, Okuno M, Ishibashi N, Hashimoto M, Yamamoto M, et al. Prevention of rat hepatocarcinogenesis by acyclic retinoid is accompanied by reduction in emergence of both TGF-alpha-expressing oval-like cells and activated hepatic stellate cells. Nutr Cancer 2005;51:197–206.
15. Muto Y, Moriwaki H, Omori M. *In vitro* binding affinity of novel synthetic polyprenoids (polyprenoic acids) to cellular retinoid-binding proteins. Gann 1981;72:974–7.
16. Yamada Y, Shidoji Y, Fukutomi Y, Ishikawa T, Kaneko T, Nakagama H, et al. Positive and negative regulations of albumin gene expression by retinoids in human hepatoma cell lines. Mol Carcinog 1994;10:151–8.
17. Honda M, Sakai A, Yamashita T, Nakamoto Y, Mizukoshi E, Sakai Y, et al. Hepatic ISG expression is associated with genetic variation in interleukin 28B and the outcome of IFN therapy for chronic hepatitis C. Gastroenterology 2010;139:499–509.
18. Frith C, Ward J, Turusov V. Pathology of tumors in laboratory animals. Vol. 2. Lyon, France: IARC Scientific Publications; 1994. p. 223–70.
19. Thoolen B, Maronpot RR, Harada T, Nyska A, Rousseaux C, Nolte T, et al. Proliferative and nonproliferative lesions of the rat and mouse hepatobiliary system. Toxicol Pathol 2010;38: 5S–81S.
20. Honda M, Takehana K, Sakai A, Tagata Y, Shirasaki T, Nishitani S, et al. Malnutrition impairs interferon signaling through mTOR and FoxO pathways in patients with chronic hepatitis C. Gastroenterology 2011;141:128–40, 140.e1–2.
21. Frith CH, Ward JM, Turusov VS. Tumours of the liver. IARC Sci Publ 1994;111:223–69.
22. Xu L, Hui AY, Albanis E, Arthur MJ, O'Byrne SM, Blaner WS, et al. Human hepatic stellate cell lines, LX-1 and LX-2: new tools for analysis of hepatic fibrosis. Gut 2005;54:142–51.
23. Nhieu JT, Renard CA, Wei Y, Cherqui D, Zafrani ES, Buendia MA. Nuclear accumulation of mutated beta-catenin in hepatocellular carcinoma is associated with increased cell proliferation. Am J Pathol 1999;155:703–10.
24. Wong CM, Fan ST, Ng IO. beta-Catenin mutation and overexpression in hepatocellular carcinoma: clinicopathologic and prognostic significance. Cancer 2001;92:136–45.
25. van Zijl F, Mair M, Csiszar A, Schneller D, Zulehner G, Huber H, et al. Hepatic tumor-stroma crosstalk guides epithelial to mesenchymal transition at the tumor edge. Oncogene 2009;28: 4022–33.
26. Fischer AN, Fuchs E, Mikula M, Huber H, Beug H, Mikulits W. PDGF essentially links TGF-beta signaling to nuclear beta-catenin accumulation in hepatocellular carcinoma progression. Oncogene 2007;26: 3395–405.
27. Hou X, Kumar A, Lee C, Wang B, Arjunan P, Dong L, et al. PDGF-CC blockade inhibits pathological angiogenesis by acting on multiple cellular and molecular targets. Proc Natl Acad Sci U S A 2010;107: 12216–21.
28. Apte U, Zeng G, Muller P, Tan X, Micsenyi A, Cieply B, et al. Activation of Wnt/beta-catenin pathway during hepatocyte growth factor-induced hepatomegaly in mice. Hepatology 2006;44:992–1002.
29. Eguchi S, Kanematsu T, Arii S, Omata M, Kudo M, Sakamoto M, et al. Recurrence-free survival more than 10 years after liver resection for hepatocellular carcinoma. Br J Surg 2011;98:552–7.
30. Okusaka T, Ueno H, Ikeda M, Morizane C. Phase I and pharmacokinetic clinical trial of oral administration of the acyclic retinoid NIK-333. Hepatol Res 2011;41:542–52.
31. Okusaka T, Makuuchi M, Matsui O, Kumada H, Tanaka K, Kaneko S, et al. Clinical benefit of peretinoin for the suppression of hepatocellular carcinoma (HCC) recurrence in patients with Child-Pugh grade A (CP-A) and small tumor: a subgroup analysis in a phase II/III randomized, placebo-controlled trial. J Clin Oncol 2011;29 Suppl 4s:165.
32. Araki H, Shidoji Y, Yamada Y, Moriwaki H, Muto Y. Retinoid agonist activities of synthetic geranyl geranoic acid derivatives. Biochem Biophys Res Commun 1995;209:66–72.
33. Nakamura N, Shidoji Y, Yamada Y, Hatakeyama H, Moriwaki H, Muto Y. Induction of apoptosis by acyclic retinoid in the human hepatoma-derived cell line, HuH-7. Biochem Biophys Res Commun 1995;207: 382–8.
34. Yasuda I, Shiratori Y, Adachi S, Obora A, Takemura M, Okuno M, et al. Acyclic retinoid induces partial differentiation, down-regulates telomerase reverse transcriptase mRNA expression and telomerase activity, and induces apoptosis in human hepatoma-derived cell lines. J Hepatol 2002;36:660–71.
35. Tatsukawa H, Sano T, Fukaya Y, Ishibashi N, Watanabe M, Okuno M, et al. Dual induction of caspase 3- and transglutaminase-dependent apoptosis by acyclic retinoid in hepatocellular carcinoma cells. Mol Cancer 2011;10:4.
36. Timke C, Zieher H, Roth A, Hauser K, Lipson KE, Weber KJ, et al. Combination of vascular endothelial growth factor receptor/platelet-derived growth factor receptor inhibition markedly improves radiation tumor therapy. Clin Cancer Res 2008;14: 2210–9.
37. Molander C, Hackzell A, Ohta M, Izumi H, Funa K. Sp1 is a key regulator of the PDGF beta-receptor transcription. Mol Biol Rep 2001;28: 223–33.
38. Bonello MR, Khachigian LM. Fibroblast growth factor-2 represses platelet-derived growth factor receptor-alpha (PDGFR-alpha) transcription via ERK1/2-dependent Sp1 phosphorylation and an atypical cis-acting element in the proximal PDGFR-alpha promoter. J Biol Chem 2004;279:2377–82.
39. Komi Y, Sogabe Y, Ishibashi N, Sato Y, Moriwaki H, Shimokado K, et al. Acyclic retinoid inhibits angiogenesis by suppressing the MAPK pathway. Lab Invest 2010;90:52–60.

40. Shah S, Hecht A, Pestell R, Byers SW. Trans-repression of beta-catenin activity by nuclear receptors. J Biol Chem 2003;278: 48137–45.
41. Kitareewan S, Blumen S, Sekula D, Bissonnette RP, Lamph WW, Cui Q, et al. G0S2 is an all-trans-retinoic acid target gene. Int J Oncol 2008;33:397–404.
42. Uray IP, Shen Q, Seo HS, Kim H, Lamph WW, Bissonnette RP, et al. *Rexinoid-induced expression of IGFBP-6 requires RARbeta-dependent* permissive cooperation of retinoid receptors and AP-1. J Biol Chem 2009;284:345–53.
43. Hough S, Avioli LV, Muir H, Gelderblom D, Jenkins G, Kurasi H, et al. Effects of hypervitaminosis A on the bone and mineral metabolism of the rat. Endocrinology 1988;122: 2933–9.
44. Ribaya-Mercado JD, Blumberg JB. Vitamin A: is it a risk factor for osteoporosis and bone fracture? Nutr Rev 2007;65: 425–38.
45. Llovet JM, Ricci S, Mazzaferro V, Hilgard P, Gane E, Blanc JF, et al. Sorafenib in advanced hepatocellular carcinoma. N Engl J Med 2008;359:378–90.
46. Okita K, Matsui O, Kumada H, Tanaka K, Kaneko S, Moriwaki H, et al. Effect of peretinoin on recurrence of hepatocellular carcinoma (HCC): results of a phase II/III randomized placebo-controlled trial. J Clin Oncol 2010;28 Suppl 15s:4024.